Finding Pattern in the Noise: Persistent Implicit Statistical Knowledge Impacts the Processing of Unpredictable Stimuli

Andrea Kóbor, Karolina Janacsek, Petra Hermann, Zsófia Zavecz, Vera Varga, Valéria Csépe, Zoltán Vidnyánszky, Gyula Kovács, Dezso Nemeth

Finding Pattern in the Noise: Persistent Implicit Statistical Knowledge Impacts the Processing of Unpredictable Stimuli

Andrea Kóbor[1*], Karolina Janacsek[2,3*], Petra Hermann[1], Zsófia Zavecz[4], Vera Varga[1,5], Valéria Csépe[1,5], Zoltán Vidnyánszky[1], Gyula Kovács[6], and Dezso Nemeth[7,8,9]

Abstract

■ Humans can extract statistical regularities of the environment to predict upcoming events. Previous research recognized that implicitly acquired statistical knowledge remained persistent and continued to influence behavior even when the regularities were no longer present in the environment. Here, in an fMRI experiment, we investigated how the persistence of statistical knowledge is represented in the brain. Participants (n = 32) completed a visual, four-choice, RT task consisting of statistical regularities. Two types of blocks constantly alternated with one another throughout the task: predictable statistical regularities in one block type and unpredictable ones in the other. Participants were unaware of the statistical regularities and their changing distribution across the blocks. Yet, they acquired the statistical regularities and showed significant statistical knowledge at the behavioral level not only in the predictable blocks but also in the unpredictable ones, albeit to a smaller extent. Brain activity in a range of cortical and subcortical areas, including early visual cortex, the insula, the right inferior frontal gyrus, and the right globus pallidus/putamen contributed to the acquisition of statistical regularities. The right insula, inferior frontal gyrus, and hippocampus as well as the bilateral angular gyrus seemed to play a role in maintaining this statistical knowledge. The results altogether suggest that statistical knowledge could be exploited in a relevant, predictable context as well as transmitted to and retrieved in an irrelevant context without a predictable structure. ■

INTRODUCTION

The extraction and acquisition of statistical regularities underlying the sensory input enables us to make predictions in noisy environments (Bubic, Von Cramon, & Schubotz, 2010). By repeatedly sampling this input, statistical regularities are usually acquired implicitly and without intention (Vékony, Ambrus, Janacsek, & Nemeth, 2022; Conway, 2020; Frost, Armstrong, & Christiansen, 2019; Aslin, 2017). However, if the regularities of the sensory input change, predictions built upon the former statistical knowledge are challenged (Qian, Jaeger, & Aslin, 2012; Bar, 2007). Interestingly, acquired statistical knowledge seems to be persistent, with people relying on that knowledge even when it is no longer relevant (Horváth, Nemeth, & Janacsek, 2022; Kóbor, Janacsek, Takács, & Nemeth, 2017; Szegedi-Hallgató et al., 2017; Bulgarelli & Weiss, 2016; Karuza et al., 2016). For example, in our previous behavioral work (Kóbor, Horváth, Kardos, Nemeth, & Janacsek, 2020), participants first encountered a predictable statistical structure consisting of biased probabilities, followed by unpredictable stimuli consisting of equal probabilities. Not only did they acquire the predictable probabilities but also showed a similar learning effect for the unpredictable stimuli. Although persistent statistical knowledge has been shown behaviorally, it is not yet fully understood how this persistence is represented in the brain. Therefore, in the present fMRI experiment, we investigated brain activity underlying the persistence of implicit statistical knowledge in a context where this knowledge is irrelevant.

The neural background of acquiring statistical regularities has been investigated in both the auditory and the visual domains extensively (for reviews, see Conway, 2020; Janacsek et al., 2020; Batterink, Paller, & Reber, 2019; Hardwick, Rottschy, Miall, & Eickhoff, 2013; Reber, 2013). On the basis of the evidence accumulated so far, this acquisition mechanism has been found to rely on a network of cortical and subcortical areas, including the medial temporal lobe, the basal ganglia, and the cerebellum (e.g., Janacsek et al., 2022; Park, Janacsek, Nemeth, & Jeon, 2022; Ma et al., 2021; Magon et al., 2020; Karlaftis et al., 2019; Albouy, King, Maquet, & Doyon, 2013;

[1]Brain Imaging Centre, HUN-REN Research Centre for Natural Sciences, Hungary, [2]Centre of Thinking and Learning, Institute for Lifecourse Development, School of Human Sciences, University of Greenwich, United Kingdom, [3]ELTE Eötvös Loránd University, Hungary, [4]University of Cambridge, United Kingdom, [5]University of Pannonia, Hungary, [6]Friedrich Schiller University Jena, Germany, [7]INSERM, CRNL U1028 UMR5292, France, [8]ELTE Eötvös Loránd University & HUN-REN Research Centre for Natural Sciences, Hungary, [9]University of Atlántico Medio, Spain
*These authors contributed equally to this work.

Rieckmann, Fischer, & Backman, 2010; Turk-Browne, Scholl, Johnson, & Chun, 2010; Doyon et al., 2009; Turk-Browne, Scholl, Chun, & Johnson, 2009; Schendan, Searl, Melrose, & Stern, 2003; Willingham, Salidis, & Gabrieli, 2002; Bischoff-Grethe, Martin, Mao, & Berns, 2001). Although the acquisition of statistical regularities in the brain has been widely explored, the neural underpinnings responsible for the persistence of the acquired statistical knowledge remain less clear.

Considering the applied paradigms and designs, neuroimaging studies on the acquisition of visuomotor statistical regularities have typically contrasted blocks of sequenced and random stimuli alternating throughout the task (e.g., Dennis & Cabeza, 2011; Rieckmann et al., 2010; Poldrack et al., 2005; Schendan et al., 2003). In these studies, the typical analysis of the sequenced > random contrast revealed which brain regions were involved in the acquisition of statistical regularities and in the use of this knowledge when relevant, that is, when statistical regularities were indeed predictable. The present fMRI study, using a visuomotor, four-choice SRT task, goes beyond the existing ones in the following way. Here, the distribution of statistical regularities is either predictable (biased probabilities) or unpredictable (equal probabilities) in two different, quickly alternating blocks. Hence, statistical knowledge obtained in the predictable blocks becomes irrelevant in the other, unpredictable blocks. Regarding the modulation of relevance, unpredictable blocks help us to probe the persistence of the obtained statistical knowledge. Therefore, in addition to contrasting predictable and unpredictable blocks, we also analyze the brain activity associated with the behavioral score of statistical knowledge observed separately in the two block types.

For this experiment, we assumed that the brain regions supporting the acquisition of biased statistical regularities would show increased predictable > unpredictable activity associated with higher statistical knowledge score in the predictable blocks. On the basis of our earlier behavioral study, it was expected that statistical knowledge acquired in the predictable blocks would be further applied in the unpredictable blocks (Kóbor et al., 2020). This would be evidenced by a significant statistical knowledge score at the behavioral level, not only in the predictable blocks but also in the unpredictable ones. Importantly, because there were no learnable (biased) statistical regularities in the unpredictable blocks, statistical knowledge observed in these blocks would be acquired in and transmitted from only the predictable blocks. Because the different types of blocks alternated rapidly, the acquisition, generalization, retrieval, and application of statistical knowledge might not have been dissociable processes; instead, it is likely that they continuously built upon each other during task performance. Following this logic, we investigated the persistence of statistical knowledge from predictable to unpredictable blocks using various measures of the brain–behavior relationship.

First, we assumed that brain regions where increased predictable > unpredictable activity is associated with higher statistical knowledge score in the unpredictable blocks would support the continuous transmission of statistical knowledge from predictable to unpredictable blocks. Second, brain regions where increased unpredictable > predictable activity is associated with higher statistical knowledge score in the unpredictable blocks would contribute uniquely and specifically to the persistence of statistical knowledge in the unpredictable blocks. Third, brain regions where increased brain activity separately in the unpredictable blocks is associated with higher statistical knowledge score in the same blocks would support the implicit retrieval and application of the generalized statistical knowledge. We focused on these contrasts to reveal the different elements of generalization and persistence.

In terms of the hypotheses regarding the specific brain regions, we expected that greater basal ganglia activation would be coupled with increased statistical knowledge in the predictable blocks. This hypothesis was based on a recent activation likelihood estimation meta-analysis (Janacsek et al., 2020), showing a strong link between basal ganglia and learning in visuomotor SRT tasks. We also expected increased hippocampal activity associated with increased statistical knowledge in the predictable blocks. The hippocampus has been shown to be active when learning statistical regularities and anticipating predictive sequences (e.g., Forest, Schlichting, Duncan, & Finn, 2023; Sherman & Turk-Browne, 2020; Schapiro, Turk-Browne, Botvinick, & Norman, 2017; Schapiro, Gregory, Landau, McCloskey, & Turk-Browne, 2014; Schapiro, Kustner, & Turk-Browne, 2012; Rose, Haider, Salari, & Büchel, 2011; Rieckmann et al., 2010; Turk-Browne et al., 2010; Fletcher et al., 2005; Schendan et al., 2003), as well as when consolidating, retrieving, and applying the learned statistical knowledge (Albouy et al., 2008, 2013, 2015; Ross, Brown, & Stern, 2009).

Next, we hypothesized that if statistical knowledge were transmitted across the block types, increased hippocampal activity in the predictable blocks would be coupled with greater statistical knowledge in the unpredictable blocks. The hippocampus has been found to play a role in integrating recurring information across multiple types of experiences to form generalized representations, guiding decisions in novel situations (Sherman, Turk-Browne, & Goldfarb, 2024; Zeithamova & Bowman, 2020; Keresztes, Ngo, Lindenberger, Werkle-Bergner, & Newcombe, 2018; Henke, 2010). For instance, when humans learned overlapping associations between different stimuli, the activity of the hippocampus during encoding predicted behavioral generalization performance during retrieval, even without explicit awareness of the relationships between stimuli (Shohamy & Wagner, 2008). On the basis of these findings, we assumed that similar hippocampal mechanisms would support the generalization of statistical knowledge across stimuli that were perceptually comparable. Meanwhile, we did not form a priori hypotheses on

which brain regions would support the persistence and implicit retrieval of statistical knowledge specifically in the unpredictable blocks. Altogether, the present fMRI study examined the brain regions involved in acquiring and maintaining implicit statistical knowledge.

METHODS

Participants

Forty healthy young adults took part in the study. They were recruited from university courses and via social media ads of our laboratory. Altogether, eight participants were excluded after the fMRI experiment because of the following reasons: technical problems during data acquisition yielding incomplete data ($n = 2$); not meeting the recruitment criteria, which, accidentally, was revealed only at the time of the fMRI experiment ($n = 2$); neurological malformations (e.g., cystic lesions) revealed during the scanning ($n = 3$); and very poor task performance with an accuracy below 50% ($n = 1$). Therefore, the final sample consisted of 32 participants (22 female participants) between the ages of 19 and 29 years ($M = 22.2$, $SD = 2.9$).

The sample size was determined based on three considerations. At the time of planning the present fMRI study, only behavioral data were available with experimental designs similar to this one. Therefore, we focused on reproducing the critical behavioral effects. First, we based the sample size on a separate behavioral pilot experiment that applied alternating predictable and unpredictable blocks. The length, structure, and timing of the pilot experiment were the same as that of the present fMRI experiment, except for minor modifications. It was conducted under standard laboratory conditions with the participation of 23 healthy young adults. RT results showed that statistical knowledge was significantly larger in the predictable than unpredictable blocks, which interaction effect was considered as the contrast of interest.

Second, our earlier behavioral work (Kóbor et al., 2020) indirectly influenced our decision about the sample size. In that more complex design, the predictability of task blocks changed only once, in the middle of the task, instead of alternating from block to block. The group completing the predictable blocks first showed similar statistical knowledge in both the predictable and unpredictable blocks. The group completing the unpredictable blocks first showed no statistical knowledge in the unpredictable blocks and significant knowledge in the predictable blocks. This interaction effect was significant with a sample size of 25 in each group, which guided our decision.

Third, we used a stopping rule of 30 participants to counterbalance the use of the underlying probabilistic sequences (for details, see the Experimental Task section). We continuously monitored the sample in terms of data quality (i.e., overall accuracy and motion artifacts) and counterbalancing. If a participant had to be excluded during fMRI data acquisition or after checking the data quality, we recruited another participant to replace them by paying attention to counterbalancing. Eventually, we kept data of two more participants than originally planned (see the fMRI Data Analysis section), leading to a final sample of 32 participants. On the basis of the critical behavioral effects found earlier, the sample size of 32 was regarded as sufficient to detect the significant change of statistical knowledge as a function of block predictability.

Participants were undergraduate and graduate students (years of education: $M = 15.2$, $SD = 2.3$) from various universities. Handedness was assessed with the Edinburgh Handedness Inventory revised version (Dragovic, 2004a, 2004b; Oldfield, 1971), according to which the mean laterality quotient was 62.7 ($SD = 67.7$; -100 means complete left-handedness, 100 means complete right-handedness). According to the predefined inclusion criteria, participants had normal or corrected-to-normal vision; none of them reported any history of neurological, psychiatric, or other chronic medical conditions; and none of them was taking any psychoactive medication or reported any other circumstances preventing MRI scanning. As a part of the usual participant screening procedure of our laboratory, standard neuropsychological tests were administered before the fMRI experiment in a separate session. Participants performed in the normal range on these tests (Wisconsin Card Sorting Task [perseverative error percentage]: $M = 10.88$, $SD = 2.91$; digit span task [mean short-term memory span; possible range: 3–9]: $M = 6.19$, $SD = 1.38$; counting span task [mean working memory span; possible range: 2–6]: $M = 3.41$, $SD = 0.76$; go/no-go task [discriminability index: hit rate minus false alarm rate]: $M = 0.71$, $SD = 0.18$; these results are not published elsewhere). All participants provided written informed consent before enrollment and received course credits or vouchers (equivalent to a payment of ca. 15 euros) in exchange for taking part in the study. The study was approved by the Ethical Board of the Medical Research Council, Hungary (Approval No. OGYÉI/10767/2017), and was conducted in accordance with the Declaration of Helsinki.

Experimental Task

Implicit acquisition of statistical regularities was measured by a modified version of the alternating serial reaction time (ASRT) task (Kóbor et al., 2020; Nemeth et al., 2010; Howard & Howard, 1997). In this task, four empty circles ($d = 1°$; black outline) were presented horizontally on a uniform mid-gray background with 2° between their centers. In each trial, one of the circles was filled in red (see Figure 1A). In brief, participants were instructed to indicate the position of the red stimulus by pressing one of the four spatially corresponding response keys on the ResponseGrip (NordicNeuroLab) as quickly and accurately as possible (leftmost position – left index finger, second position from left to right – left thumb, third position from left to right – right thumb, rightmost position – right

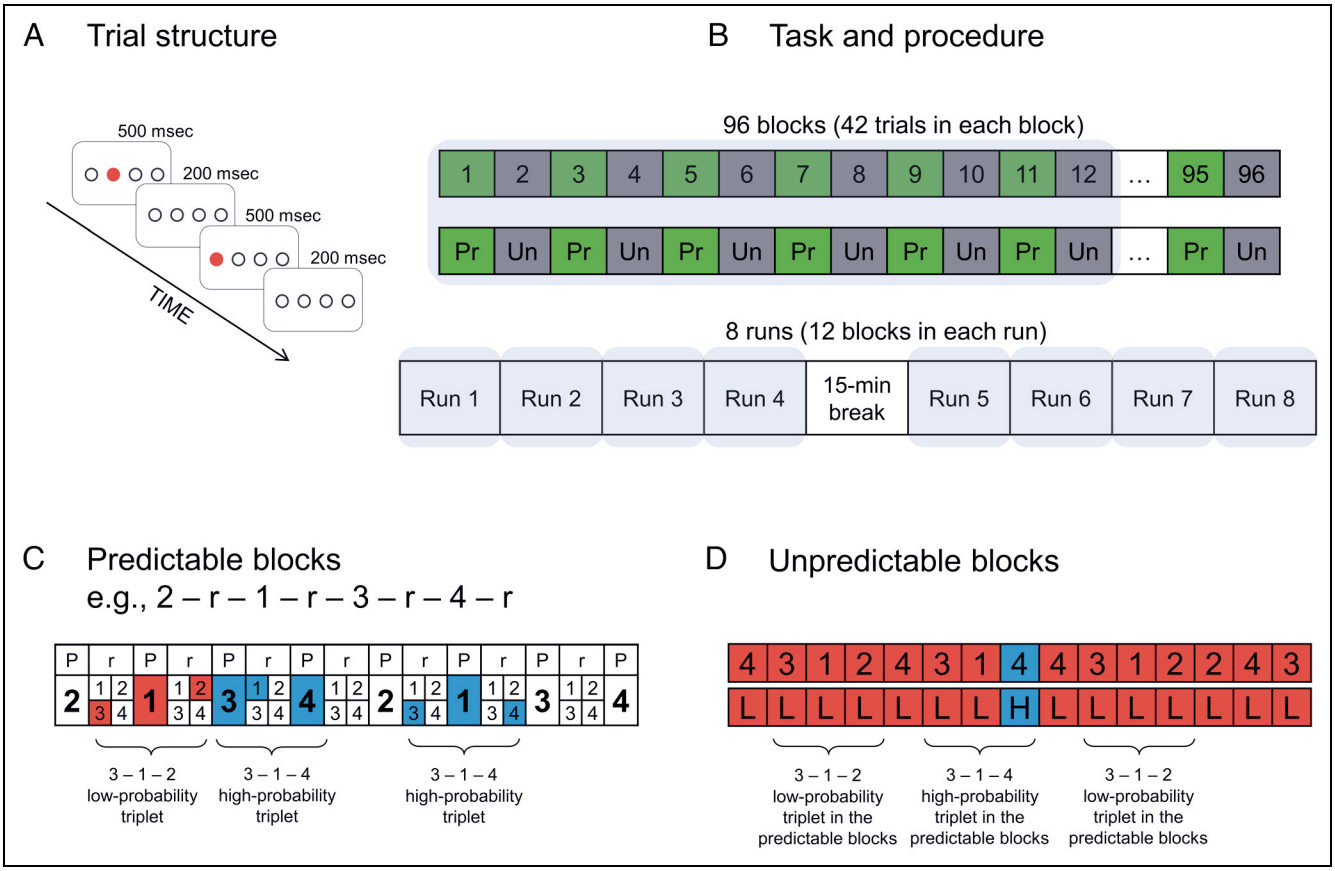

Figure 1. Design of the experiment. (A) One of the four horizontally arranged empty circles presented on the screen was filled in red in every 700 msec. Participants had to indicate the position of the red stimulus with one of the four response keys. (B) In the main task, 48 predictable (Pr) and 48 unpredictable (Un) blocks alternated with one another. It was completed in eight runs organized into two scanning sessions that were divided by a 15-min-long break. Each run consisted of 12 blocks (six predictable, six unpredictable), as denoted by the light gray shading. (C) In the predictable blocks, the presentation of the red stimuli followed an eight-element-long sequence, within which pattern (P) and random (r) elements alternated with one another. Numbers denote the four different stimulus positions on the screen. Pattern elements are indicated by one number as their positions were fixed, whereas random elements are indicated by four numbers as their positions were chosen randomly from the four possible ones. The alternating sequence makes some runs of three consecutive trials (triplets) more probable than others. This probability refers to the third trial of each triplet. However, note that triplet probability was determined for all trials in a sliding window manner, that is, the third trial of a triplet was also the second and first trial of the following triplets. High-probability triplets are denoted with blue shading, and low-probability triplets are denoted with coral shading. This coloring indicates some examples of low- and high-probability triplets that can be observed given the 2 – r – 1 – r – 3 – r – 4 – r alternating sequence. (D) In the unpredictable blocks, the alternating sequence was absent, but the same unique triplets as in the predictable blocks appeared with equal probability. Although the probability of triplets was biased only in the predictable blocks and equal in the unpredictable blocks, triplets in the unpredictable blocks are still labeled as either high or low probability according to their actual probability in the predictable blocks. Blue shading (upper row) and capital letter "H" (lower row) denote the third element of high-probability triplets; coral shading and "L" denote the third element of low-probability triplets. For each participant, at the level of unique triplets, the identified high- and low-probability triplets were the same in the unpredictable as in the predictable blocks.

index finger). More details on the instructions are presented in the Procedure section.

The timing of the experimental trials was the same as in the study of Kóbor and colleagues (2020). It started with the presentation of the red stimulus at one of the four positions for 500 msec. After stimulus offset, the four empty circles were presented for 200 msec (see Figure 1A) followed by the next red stimulus, yielding a 700-msec-long intertrial interval. The behavioral response was expected from stimulus onset until the end of the trial (i.e., for 700 msec). Importantly, the length of the trial was fixed, irrespective of whether participants provided correct, incorrect, or missing response(s), and no trial-wise feedback was presented as a function of response correctness. These characteristics ensured that each trial and each block (see below) had the same length, respectively. Although the experimental trials remained unchanged at the surface level throughout the task, the underlying regularity determining the positions of the red stimuli differed across the predictable and unpredictable blocks (see Figure 1B). As described below, block types were labeled as either predictable or unpredictable based on the actual predictability of the statistical regularities that they consisted of.

Predictable Blocks

In the predictable blocks, unbeknown to the participants, the order of positions where the red stimuli appeared (i.e., trial order) followed an eight-element-long probabilistic

sequence. In this sequence, predetermined/pattern (P) and random (r) elements alternated with one another (see Figure 1C). For instance, 2 – r – 1 – r – 3 – r – 4 – r was one of the sequences, where numbers denoted the positions on the screen from left to right and *r*s denoted randomly chosen positions. There were six unique permutations of the four positions, which served as the probabilistic sequences: 1 – r – 2 – r – 3 – r – 4 – r, 1 – r – 2 – r – 4 – r – 3 – r, 1 – r – 3 – r – 2 – r – 4 – r, 1 – r – 3 – r – 4 – r – 2 – r, 1 – r – 4 – r – 2 – r – 3 – r, and 1 – r – 4 – r – 3 – r – 2 – r. Importantly, only one sequence per participant was used throughout the predictable blocks to determine trial order. The given sequence was selected for each participant in a pseudorandom manner.

One predictable block contained 42 trials, and altogether, 48 predictable blocks were completed (2016 trials in total). The eight-element-long alternating sequence repeated five times in each block. The trials of each block were categorized as chunks of three successive trials, henceforth referred to as triplets. Particularly, each trial was categorized as the third trial of a triplet that was also the second trial of the following triplet, for example, 2 – 3 – **1**, 3 – **1** – 2 (Kóbor et al., 2021; Szegedi-Hallgató et al., 2017). The first two trials of the block were not categorized as triplets; therefore, 40 triplets were constructed in each block. However, not all of them were used in the analysis (see Behavioral Data Analysis section).

The alternating sequence yields a hidden probability structure in which the distribution of triplets is biased (see Figure 1C). In the case of the 2 – r – 1 – r – 3 – r – 4 – r sequence, 2 – X – 1, 1 – X – 3, 3 – X – 4, and 4 – X – 2 are high-probability triplets (X denotes the middle trial of the triplet) because these triplets could have both P – r – P and r – P – r structure and thereby occur more frequently during the task. However, for instance, 3 – X – 2 and 4 – X – 3 are low-probability triplets because these could only have a r – P – r structure and thereby occur less frequently (e.g., Nemeth, Janacsek, Polner, & Kovacs, 2013; Nemeth & Janacsek, 2011). In other words, random trials appear either with high or low probability, whereas pattern trials always appear with high probability.

When the triplet-level structure is considered in the task, the distributional and transitional probability characteristics of triplets completely overlap (Szegedi-Hallgató, Janacsek, & Nemeth, 2019; Kóbor et al., 2018; Szegedi-Hallgató et al., 2017). This means that the above-described frequency or occurrence probability of the triplets is the same as the probability to which the third trials of the triplets are predictable (second-order, nonadjacent dependency). Particularly, although the third trials of high-probability triplets are predictable continuations for the first trials, the third trials of low-probability triplets are less predictable continuations for the first trials. In the case of the above-mentioned sequence, if the first trial of a triplet is Position 3, it is more likely (with 62.5% probability) to be followed by Position 4 as the third trial than either Position 1, 2, or 3 (with 12.5% probability each). There are 64 possible unique triplets in the task: 16 of them are high-probability triplets, and 48 are low-probability ones. With respect to the unique triplets, the third trials of high-probability triplets are five times more predictable based on the first trials than those of the low-probability triplets.

Unpredictable Blocks

In the unpredictable blocks, unbeknown to the participants, the alternating sequence was absent, but trial order was still determined by the repetitions of the 64 unique triplets. Because each unique triplet occurred with equal probability (each 30 times) in these blocks, they were unpredictable (see Figure 1D). In terms of transitional probabilities, this meant that each position (1, 2, 3, or 4) as the third trial of a unique triplet could be expected based on the first trial with the same probability (25%). The unpredictable blocks altogether contained the same number of trials and triplets as the predictable blocks. Because of the equal probability structure, the order of trials differed between unpredictable and predictable blocks. To sum up, there were 64 possible unique triplets in both the predictable and unpredictable blocks. However, in predictable blocks, 16 of them were high-probability and 48 were low-probability triplets, whereas in unpredictable blocks, the 64 triplets were equally distributed.

Several trial sets were generated and then selected to determine trial order in the unpredictable blocks. The details of this procedure and other constraints on the trial sets (e.g., immediate repetition of a trial, the distribution of triplets) are described in Kóbor and colleagues (2020). Trials of the final trial sets were categorized as triplets following either of the six probabilistic sequences described above. For instance, in the case of a participant having the 2 – r – 1 – r – 3 – r – 4 – r sequence in the predictable blocks, the 3 – X – 4 triplet was categorized as a high-probability triplet in both the predictable and unpredictable blocks (see Figure 1D). Therefore, the analyzed high- and low-probability triplets were the same in the unpredictable and predictable blocks for each participant at the level of unique triplets. As can be seen in Figure 1C–D, the 3 – 1 – 4 triplets appeared in both block types but had high probability only in the predictable blocks. Still, for the sake of consistency, triplets in the unpredictable blocks are referred to as either high or low probability according to their actual probability in the predictable blocks.

Considering the distribution of the six unique alternating sequences, in the final sample ($n = 32$), each of the 1 – r – 2 – r – 4 – r – 3 – r and the 1 – r – 4 – r – 2 – r – 3 – r sequences were used six times, and the other four sequences were used five times. The distribution of high- and low-probability triplets did not differ across the four stimulus positions either in the predictable blocks, $\chi^2(3) = 3.03$, $p = .387$, or in the unpredictable blocks, $\chi^2(3) = 0.01$, $p = .999$, and these associations between triplet distribution and stimulus position did

not differ across the block types, Wald $\chi^2(3) = 1.48$, $p = .687$. Irrespective of triplets, the distribution of stimulus positions did not differ between the block types, $\chi^2(3) = 0.57$, $p = .903$.

Procedure

In the main task, the predictable and unpredictable blocks alternated with one another for altogether 96 task blocks, starting with a predictable block for every participant. Each block was 30.4 sec long. After completing a block, participants received feedback (lasting for 4 sec) about their mean RT and accuracy. The feedback screen was followed by a rest period with a fixation cross present for a randomized length of 10, 12, or 14 sec (mean = 12 sec). The main task was completed in eight separate runs, each composed of 12 blocks (six predictable and six unpredictable blocks; see Figure 1B).

Two practice sessions were administered before starting the main task. In the first session, participants practiced the stimulus–response mappings outside the scanner with six mini-blocks of random trials (15 trials each) that were self-paced with a 120-msec-long response-to-stimulus interval. Participants performed the second session in the scanner, which consisted of six mini-blocks of random trials (15 trials each) with the same fixed-paced fast intertrial interval and block-wise feedback as in the main task.

Because of the protracted nature of the experiment, it was conducted in two scanning sessions separated by a 15-min-long break that participants spent outside the scanner (see Figure 1B). After finishing the second practice session, the first scanning session started with a 10-min-long run for acquiring resting-state functional data (data are not analyzed here). Next, four runs of the task were administered. After the break, the second scanning session started with a structural run (6 min 24 sec), followed by the remaining four runs of the task. A central fixation cross was presented during the acquisition of the resting-state and structural data. Each task run lasted 10 min 16 sec, which also involved a 30-sec-long presentation of a fixation cross centered on a blank screen at the beginning and end of the runs. Breaks between each run lasted approximately 1 min. Altogether, the first session was approximately 55 min long and the second session was approximately 51 min long.

Participants received detailed verbal instructions about the task and the fMRI experimental procedures. The structural and timing characteristics were made transparent to them (i.e., number of runs, length of the runs, length of the break between the scanning sessions, number and length of the task blocks, and the length of the structural and resting-state scans). Participants were also informed about the content of the feedback presented between the blocks, such as mean RT and accuracy achieved in the given block and a textual request to "try to be faster," "try to be more accurate," or "keep doing in the same way" (these options were based on the actual performance). Brief written instructions overlapping with the verbal ones appeared at the beginning of each run. Importantly, participants were not informed about the hidden structure (predictability) of the task blocks and the statistical regularities at all. They were told that they were going to perform a task measuring sustained attention.

Participants had to "follow the movement of the red circle" with the response keys. The mapping between the stimulus positions and response keys was explained in the instructions, showed in person, and practiced before the main task. The experimenter emphasized that they should respond as soon as the stimulus appeared to not to miss it, because of the fast presentation rate. Participants were also told that if they responded too slowly to the given stimulus, their response could be registered as a very fast (and possibly incorrect) response to the next stimulus. Furthermore, the experimenter asked them not to correct their incorrect responses but to proceed with the trial to not to miss the next response. They were also told that the stimulus could appear multiple times successively at the same location. They were required not to talk or move at all in the scanner, only communicate with the response keys if needed to answer any questions of the experimenter. The panic button was placed at the left side of the body, near the left hand. Participants were asked to fixate when the fixation cross appeared on the screen; otherwise, no instruction about eye movements or fixation were given. Thus, they could freely move their gaze across the horizontally arranged circle positions.

After finishing fMRI data acquisition, a questionnaire was administered. Two questions assessed whether participants gained any consciously accessible knowledge about the structure of the task and the statistical regularities. Participants were asked (1) whether they noticed anything special regarding the task (2) and whether they noticed any regularity in the trial sequence (Kóbor et al., 2017, 2020; Song, Howard, & Howard, 2007). None of the participants reported noticing the alternating sequence, the presence of triplets, or any change in the sequence or in the regularities during the task. The full fMRI experimental procedure lasted about 3 hr, including administration, pre- and posttask questionnaires, and debriefing beyond the two practice sessions and fMRI data acquisition.

The experimental software was written in and controlled via MATLAB 2015a (The MathWorks Inc.) using the Psychophysics Toolbox Version 3.0.14 extensions (Brainard, 1997; Pelli, 1997). Stimuli were displayed on an MRI-compatible LCD screen (32-in. NNL LCD Monitor, NordicNeuroLab; 60-Hz refresh rate), placed at 142 cm from the participant and were viewed via a mirror attached to the top of the head coil. Neuropsychological tests were administered a few days before the fMRI scanning during a 1-hr-long session.

Imaging Parameters

A 3 T MRI scanner (MAGNETOM Prisma, Siemens Healthcare GmbH) was used with a 20-channel head–neck

receiver coil to acquire brain imaging data. To obtain functional scans, images were continuously acquired using a T2*-weighted gradient-echo EPI sequence with twofold in-plane GRAPPA (GeneRalized Autocalibrating Partial Parallel Acquisition) acceleration (Griswold et al., 2002; repetition time = 2000 msec; echo time = 30 msec; flip angle = 83°; 210 × 210 mm field of view; 70 × 70 in-plane matrix size; 3 × 3 mm in-plane resolution, 3-mm slice thickness, 36 slices, 25% slice gap). To obtain 3-D structural scans, sagittal T1-weighted images were acquired using a magnetization prepared fast gradient echo sequence (Mugler & Brookeman, 1990; repetition time = 2300 msec; echo time = 3.03 msec; field of view = 256 × 256 mm; 1-mm isotropic voxel size).

Behavioral Data Analysis

The original trial set was filtered before further analyses. First, trials with RTs below 100 msec were excluded for two reasons: (1) to eliminate longer responses ("slips") initiated as responses to the previous trials but recorded at the present trials, and (2) to eliminate rapid, impulsive responses to the given trials. Second, only those correctly responded trials were included in the analyses that also followed correct responses on the previous trials (cf. Kóbor et al., 2021) to avoid the RT-changing effect of errors on the subsequent trials (Horváth et al., 2021; Dutilh et al., 2012). We eliminated 27% of the trials because of filtering; however, the critical behavioral effects remained similar even with a less strict filtering. Apart from the first two trials, each trial was categorized as the third trial of a triplet. Because every trial is part of a triplet, the terms "trial" and "triplet" are interchangeable. Hence, the exclusion of, for instance, one triplet means the exclusion of one trial.

To track the temporal trajectory of acquiring statistical regularities, behavioral data were analyzed in a runwise manner. Thus, six-block-long bins of the data were grouped into larger time bins, yielding eight runs of predictable blocks and eight runs of unpredictable blocks. To be consistent with the block-wise analysis of the fMRI data, it was crucial to compare the block types to one another without considering the triplet type. Therefore, first, behavioral data were considered only at the level of block types. For each participant and run, median RTs were calculated from the filtered triplet set separately for the predictable and unpredictable blocks. Second, behavioral data were considered at the level of triplets within each block type to quantify triplet learning. For each participant and run, median RTs were calculated separately for the high- and low-probability triplets of the predictable and unpredictable blocks.

RTs at the level of block types were analyzed with a two-way repeated measures ANOVA with Block Type (predictable vs. unpredictable) and Run (one to eight) as within-subject factors. RTs at the level of triplet types were analyzed with a three-way repeated measures ANOVA with Block Type (predictable vs. unpredictable), Triplet (high- vs. low-probability), and Run (one to eight) as within-subject factors. In all ANOVAs performed on the behavioral data, the Greenhouse–Geisser epsilon (ε) correction (Greenhouse & Geisser, 1959) was used if sphericity was violated, as indicated by the significance of the Mauchly's sphericity test. Original *df* values and corrected *p* values (if applicable) are reported together with partial eta-squared (η_p^2) as the measure of effect size. Least significant difference tests for pairwise comparisons were used to control for Type I error. These statistical analyses were carried out with the Statistical Package for the Social Sciences Version 22 (IBM SPSS Statistics).

To connect the levels of behavioral measures and brain activity, first, runwise performance scores were calculated as the RT difference between the block types (RTs in unpredictable blocks minus RTs in predictable blocks) in each run. An *overall performance score* was also determined as the mean of the runwise performance scores. Second, runwise statistical knowledge scores were calculated for each block type as the RT difference between the triplet types (RTs to low-probability minus RTs to high-probability triplets) in each run. *Overall statistical knowledge scores* were determined for the predictable and unpredictable blocks, respectively, as the mean of the runwise statistical knowledge scores. The overall performance score can be considered as a noisy performance indicator likely involving some statistical knowledge as well as nonspecific processes that support task solving in the structurally different block types. Meanwhile, statistical knowledge scores directly indicate statistical knowledge. Hence, the overall performance score and the overall statistical knowledge scores of each block type were used in the fMRI analyses (see the multiple regressions below).

We also analyzed the accuracy of responses similarly to RTs. However, in this case, the trial set was not filtered based on RT or response correctness. Accuracy was first calculated as the mean ratio of correct responses for each participant, run, and block type. Second, it was determined also for high- and low-probability triplets separately within each run and block type. Beyond examining the acquisition of statistical regularities, the analysis of accuracy was also important to rule out fatigue effects and to unveil whether participants stayed focused until the end of the task. Accuracy (see Appendix) and RT findings (see the Results section) altogether suggest that the protracted nature of the experiment did not deteriorate but improved performance. Note that the fMRI analyses were connected only to the RTs and the behavioral effects discussed are also RT related, because the analysis of accuracy was not the focus of the study.

fMRI Data Analysis

Preprocessing and First-level (Single-subject) Analysis

fMRI data preprocessing and analysis were performed using SPM12 (Wellcome Trust Centre for Neuroimaging,

Institute of Neurology, University College London) running under MATLAB 2015a. Preprocessing included the following steps. First, to correct for head movements, the functional images were realigned to spatially match the mean image created after a realignment to the first scan (i.e., the first scan from each run was aligned to the first scan of the first run, and then, images within each run were aligned to the first image of the run). Second, the structural images were co-registered to the mean functional images. Third, the structural images were normalized to the Montreal Neurological Institute (MNI) template brain image (ICBM152). The deformation field parameters obtained during this step were applied to spatially normalize the realigned functional images to MNI space. Fourth, the normalized functional images were spatially smoothed with an 8-mm FWHM isotropic Gaussian kernel.

Finally, for further denoising, the preprocessed functional images were examined using the functional_art (Artifact Detection Tools, https://web.mit.edu/swg/art/art.pdf) modular function of the CONN toolbox (www.nitrc.org/projects/conn/; Power et al., 2014; Whitfield-Gabrieli & Nieto-Castanon, 2012). For each participant, outlier scans across all runs were identified by assessing scan-to-scan differences in the global BOLD signal (normalized to z scores, threshold: 5) and in composite motion (movement threshold: 0.9 mm). Outlier scans were omitted by defining a single regressor for each of them (one for the to-be-removed scans, zeros elsewhere) in the individual first-level analysis described next. The mean percentage of such outlier scans was 1.99% (SD = 1.87, range: 0.08–6.90).

Preprocessed data were analyzed using a general linear model during the individual first-level statistical analysis. Predictable and unpredictable blocks were defined as separate regressors. The regressor was a boxcar function starting at block onset and lasting for the duration of the block (30.4 sec), convolved with the canonical hemodynamic response function of SPM12. The default high-pass filter with 128-sec cutoff was used to eliminate low-frequency components, and temporal autocorrelations were accounted for by the default autoregressive AR(1) model. Motion-related variance was accounted for by including the Friston24 regressors (polynomial and temporal expansions of the six realignment parameters resulting from the realignment procedure; see Friston, Williams, Howard, Frackowiak, & Turner, 1996) and the regressors for outlier scans as covariates in the general linear model.

Second-level (Multisubject) Analyses

First, the first-level contrast images of the parameter estimates (β values) for the predictable and unpredictable blocks (predictable > unpredictable and unpredictable > predictable) were entered into the second-level, whole-brain, random-effects statistical analysis. Significance testing of the second-level t-map was performed using voxel-level false discovery rate (FDR) at q = 0.05 as correction for multiple comparisons within the gray matter mask and with a minimum cluster extent of five voxels (see the last paragraph of this section for the explanation of this extent threshold).

Second, associations between behavioral measures and brain activity were tested. Whole-brain, random-effects multiple regression analyses were performed using the individual predictable > unpredictable, unpredictable > predictable, and unpredictable > rest contrast images. The overall performance score (RT difference of predictable vs. unpredictable blocks) was entered as a second-level covariate of interest into a regression where the predictable > unpredictable contrast was used. This regression could reveal which brain areas show larger activity in the predictable than unpredictable blocks as a function of increased overall performance. The overall statistical knowledge score (RT difference of high- vs. low-probability triplets) determined for the predictable blocks was entered into a next regression where, again, the predictable > unpredictable contrast was used. This regression could reflect which brain areas support the acquisition of statistical knowledge.

The overall statistical knowledge score determined for the unpredictable blocks was entered into a separate group of regression analyses. This included three regressions focusing on different aspects of the generalization and persistence of acquired statistical knowledge. First, the predictable > unpredictable contrast, indicating brain activity specific to the predictable blocks, was used to test which brain areas support the continuous transmission of statistical knowledge across the different block types. Second, the unpredictable > predictable contrast, indicating brain activity specific to the unpredictable blocks, was used to examine which brain areas contribute uniquely to the persistence of statistical knowledge. Third, the unpredictable > rest contrast, indicating brain activity in the unpredictable blocks during task performance, was used to unveil which brain areas contribute to the retrieval and application of the generalized statistical knowledge. In all regressions described above, the behavioral scores were mean centered.

In the regressions, in order not to overlook any potential activations, the significance testing of associations was performed with a liberal threshold of p uncorrected = .001 at voxel level and with a minimum cluster extent of five voxels. We deliberately chose a small cluster extent to capture activity in the subcortical/deep brain structures where we expected significant activations. However, the standard fMRI data acquisition and analysis techniques could easily lead to cortical biases, which hinder the exploration of activity in the subcortical/deep brain structures (Janacsek et al., 2022; Lewis, Setsompop, Rosen, & Polimeni, 2018; de Hollander, Keuken, & Forstmann, 2015; Ances et al., 2008). Most importantly, only a few voxels cover these structures, and even within these voxels, the functional heterogeneity (specificity) is greater than in the cortical

structures (Haak & Beckmann, 2020). The small number of voxels might not survive the usual corrections based on cluster extent. Thus, lowering the analysis thresholds has been a common practice in earlier studies probing statistical-sequence learning, especially when focusing on activations in the basal ganglia and/or the hippocampus. For instance, even five voxels (Turk-Browne et al., 2009, 2010; Daselaar, Rombouts, Veltman, Raaijmakers, & Jonker, 2003) and six voxels (Purdon, Waldie, Woodward, Wilman, & Tibbo, 2011) as minimum cluster extent thresholds appeared in the relevant literature in regard to whole-brain or ROI analyses. The number of activated voxels in the hippocampus has also been around 10 at an uncorrected threshold of $p = .001$ without extent threshold (Albouy et al., 2015). We decided not to perform ROI analyses in relation to the subcortical/deep brain structures. First, anatomically defined masks might not have been sufficiently specific to find significant activations related to our research questions. Second, although multiple activation clusters reported in the literature could be used for defining the ROIs, these were found examining structurally different paradigms. Altogether, we used the less stringent criteria in significance testing described above, to explore subcortical/deep brain structures that potentially support the acquisition and generalization of statistical regularities at the behavioral level.

RESULTS

Behavioral Results

Overall Performance at the Level of Block Types

The Block Type × Run ANOVA on the RTs revealed significant main effects of Block Type, $F(1, 31) = 99.87$, $p < .001$, $\eta_p^2 = .763$, and Run, $F(7, 217) = 21.02$, $\varepsilon = .564$, $p < .001$, $\eta_p^2 = .404$, whereas their interaction was nonsignificant, $F(7, 217) = 1.63$, $\varepsilon = .675$, $p = .159$, $\eta_p^2 = .050$. The significant main effects indicate faster RTs in the predictable than in the unpredictable blocks ($M = 375.1$ msec, $SD = 41.3$ vs. $M = 381.8$ msec, $SD = 41.6$) and faster RTs as the task progresses. Because participants responded to unpredictable stimuli more slowly, it is likely that they became sensitive to the changes of stimulus predictability. The next analysis investigates whether sensitivity to the biased triplet probabilities has also emerged, which eventually results in the participants' discrimination of block types.

Triplet Learning

In line with the results of the previous ANOVA, the Block Type × Triplet × Run ANOVA on the RTs revealed significant main effects of Block Type, $F(1, 31) = 39.78$, $p < .001$, $\eta_p^2 = .562$, and Run, $F(7, 217) = 21.31$, $\varepsilon = .593$, $p < .001$, $\eta_p^2 = .407$. RTs were faster in the predictable than in the unpredictable blocks, and, in terms of the trajectory, they generally became faster because of practice until Run_5 ($ps \leq .047$) and did not change across $Runs_{6–8}$ ($ps \geq .403$; cf. Figure 2A–B). The change of RTs throughout the task did not differ significantly between the predictable and unpredictable blocks, Block Type × Run interaction, $F(7, 217) = 1.25$, $\varepsilon = .672$, $p = .291$, $\eta_p^2 = .039$.

More importantly, this ANOVA revealed a significant main effect of Triplet, $F(1, 31) = 38.27$, $p < .001$, $\eta_p^2 = .552$, indicating faster RTs to high-probability than to low-probability triplets ($M = 375.5$ msec, $SD = 40.3$ vs. $M = 381.8$ msec, $SD = 42.1$; cf. Figure 2A–B). This means that participants acquired statistical knowledge by triplet learning. However, the significant Block Type × Triplet interaction, $F(1, 31) = 16.98$, $p < .001$, $\eta_p^2 = .354$, revealed that the overall statistical knowledge score (i.e., the difference of low- vs. high-probability triplets) was higher in the predictable than in the unpredictable blocks. In particular, triplet learning based on the effect size measures was almost 2.5 times larger in the predictable ($M = 8.4$ msec, $SD = 5.8$, $t(31) = 8.24$, $p < .001$, $d = 1.46$), than in the unpredictable blocks ($M = 4.1$ msec, $SD = 7.1$, $t(31) = 3.31$, $p = .002$, $d = 0.59$) (see Figure 2C). Although RTs to both high- and low-probability triplets were significantly slower in the unpredictable than in the predictable blocks ($ps \leq .003$), this slowing was more pronounced for the high-probability (6.3 msec) than for the low-probability triplets (2.0 msec; see Figure 2D). This way, RTs to high- and low-probability triplets became more similar in the unpredictable blocks, decreasing the overall statistical knowledge score.

The Triplet × Run interaction was also significant, $F(7, 217) = 2.19$, $p = .036$, $\eta_p^2 = .066$, indicating that the statistical knowledge score increased throughout the task (from 3.4 msec in Run_1 to its maximum, 9.2 msec in Run_7, $p = .020$). The Block Type × Triplet × Run interaction was nonsignificant, $F(7, 217) = 0.58$, $p = .772$, $\eta_p^2 = .018$, suggesting that the learning trajectory across the runs was similar in the two block types. However, we analyzed larger temporal chunks, the first ($Runs_{1–4}$) and second ($Runs_{5–8}$) halves of the task in each block type. We performed this analysis for the following reasons. First, visual inspection of the behavioral data suggested that statistical learning occurred in the unpredictable blocks in the second half of the task (see Figure 2), which we wanted to verify statistically. Second, the 15-min-long break necessary between the scanning sessions might have influenced the results by helping the dissipation of fatigue or reducing reactive inhibition (Kóbor et al., 2019; Török, Janacsek, Nagy, Orbán, & Nemeth, 2017; Pan & Rickard, 2015). Third, the 15-min-long break can be considered as an offline learning period, which could support the stabilization and long-term retention of memories (Tóth-Fáber, Nemeth, & Janacsek, 2023; Krakauer & Shadmehr, 2006; Robertson, Pascual-Leone, & Miall, 2004), even if it was short (Szücs-Bencze et al., 2023; Bönstrup et al., 2019; Du, Prashad, Schoenbrun, & Clark, 2016).

As per the result, the statistical knowledge score across the two task halves increased significantly in both block

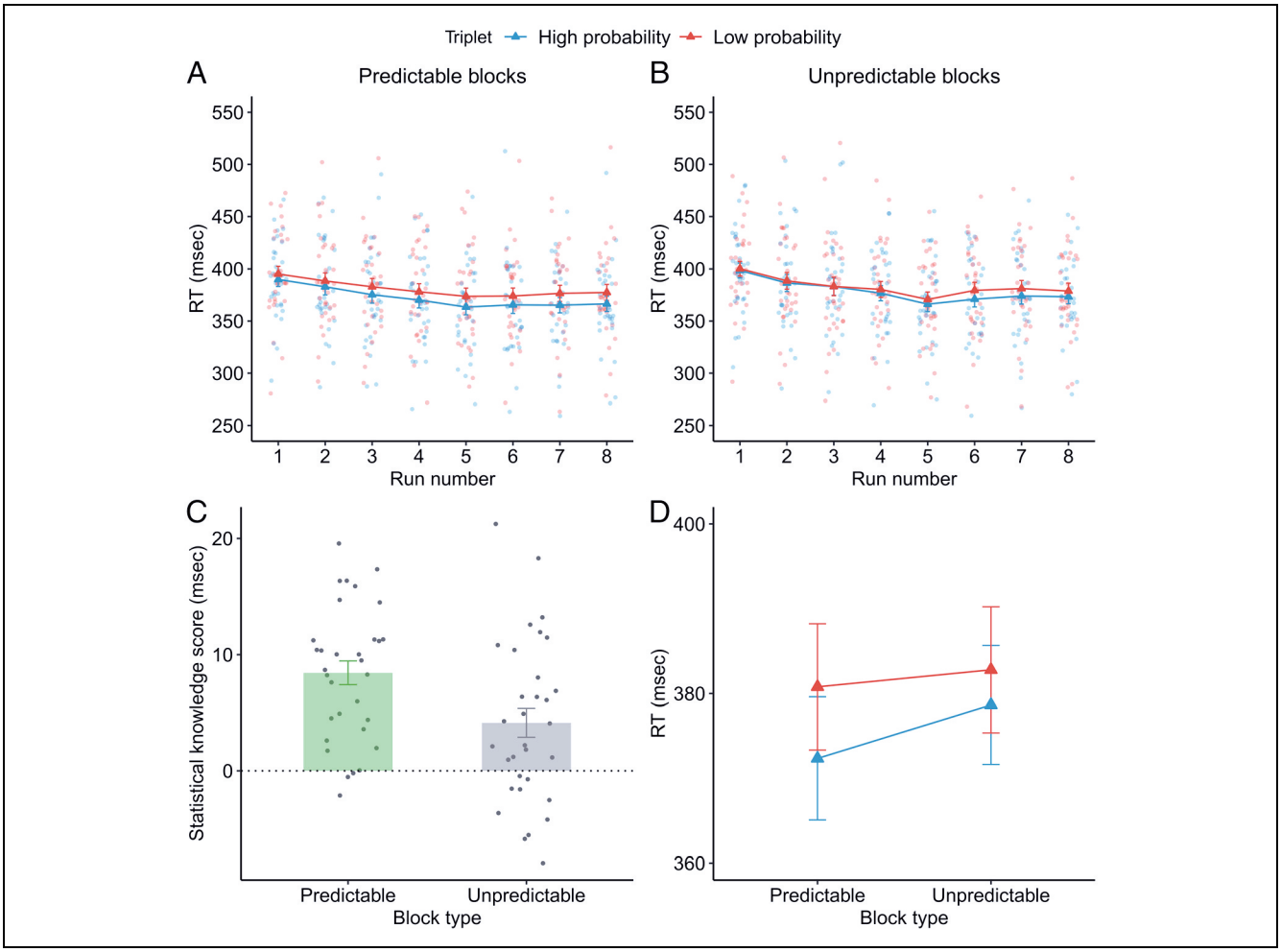

Figure 2. Behavioral results. RTs of correctly responded triplets split by run (one to eight) and triplet type (high-probability [blue] vs. low-probability [coral] triplets according to their actual probability in the predictable blocks) are presented in the predictable (A) and unpredictable (B) blocks. Triangles denote the group mean of each condition combination (run and triplet), circles denote individual data points jittered to prevent overlap, and error bars denote standard error of mean in all figure parts. Figure Part C shows the overall statistical knowledge scores (RTs to low- minus RTs to high-probability triplets, averaged across runs) separately in the predictable and unpredictable blocks. Figure Part D shows the RTs to high- and low-probability triplets averaged across runs separately in each block type.

types: from 6.6 msec to 10.3 msec in the predictable blocks, $t(31) = 2.42$, $p = .021$, and from 1.9 msec to 6.4 msec in the unpredictable blocks, $t(31) = 2.72$, $p = .011$. However, the level of triplet learning was different in the two block types: In the predictable blocks, triplet learning was significantly above zero in both the first, $t(31) = 5.48$, $p < .001$, and second task halves, $t(31) = 7.67$, $p < .001$. In contrast, in the unpredictable blocks, triplet learning was significantly above zero only in the second task half, $t(31) = 5.09$, $p < .001$, and nonsignificant in the first task half, $t(31) = 1.10$, $p = .281$.

These results altogether suggest that the equally distributed triplets in the unpredictable blocks were responded according to the statistical knowledge acquired in the predictable blocks. It is conceivable that statistical knowledge emerged gradually in the predictable blocks where it was relevant, and, after some time, it was generalized to and applied in the unpredictable blocks where it was otherwise irrelevant. This is supported by the finding that statistical knowledge in the unpredictable blocks became significant only in the second half of the task.

fMRI Results

For all fMRI results, the test statistics, p values, and characteristics of the activation clusters are presented in the tables (Tables 1–4).

Whole-brain Analysis of Block Predictability

The results of the whole-brain analysis showed significantly larger fMRI responses to the predictable than to the unpredictable blocks bilaterally in the superior and middle occipital gyrus extending to the right and left lingual gyrus around the calcarine fissure. In addition, significantly larger fMRI responses were found in the anterior lobe of the right cerebellum, in the left posterior vermis, and in the left somatosensory cortex (postcentral gyrus),

Table 1. Brain Regions Showing fMRI Responses to the Predictable versus Unpredictable Blocks

		Cluster Level	*Voxel Level*		*MNI Coordinates (mm)*		
Region		*Cluster size*	*p(FDR)*	*t Value*	*x*	*y*	*z*
Predictable > unpredictable							
Superior occipital gyrus/calcarine/cuneus	R	611	.004	6.71	14	−96	18
Superior/middle occipital gyrus/cuneus	L	276	.008	5.49	−16	−96	18
Postcentral gyrus/inferior parietal gyrus	L	16	.016	4.81	−54	−18	52
Cuneus/superior occipital gyrus	L	10	.036	4.15	−12	−88	36
Cerebellum, lobule IV, V	R	20	.036	4.15	24	−48	−24
Cerebellum, lobule VI, vermis	L	5	.043	4.00	−4	−64	−24
Middle occipital gyrus	R	5	.043	3.99	34	−92	8
Calcarine	L	8	.043	3.97	−2	−74	12
Unpredictable > predictable							
White matter/middle temporal gyrus	R	36	.045	5.62	42	−52	8
Precuneus	L	65	.045	5.18	−6	−60	52
Precuneus	R	74	.045	5.07	8	−58	56
Superior temporal gyrus	L	5	.045	4.91	−46	−44	18

The peak MNI coordinates are reported. Anatomical labels were assigned from the AAL3 atlas (Rolls, Huang, Lin, Feng, & Joliot, 2020) using the xjView 10.0 toolbox (https://www.alivelearn.net/xjview). L = left hemisphere; R = right hemisphere.

Table 2. Brain Regions Showing Positive Associations between fMRI Responses to Predictable > Unpredictable Blocks and Overall Performance Score

		Cluster Level	*Voxel Level*		*MNI Coordinates (mm)*		
Region		*Cluster Size*	*p(Uncorrected)*	*t Value*	*x*	*y*	*z*
Insula/Rolandic operculum	L	158	<.001	5.10	−40	−8	6
Insula	L	98	<.001	4.58	−30	12	8
Insula/Rolandic operculum	R	288	<.001	4.55	38	−12	8
Superior temporal gyrus/Rolandic operculum	L	97	<.001	4.49	−60	0	−4
Rolandic operculum	R	23	<.001	4.03	64	−2	8
Superior/middle temporal gyrus	L	25	<.001	4.00	−58	−34	10
Supramarginal gyrus	R	62	<.001	3.92	50	−34	24
Inferior temporal gyrus	R	6	<.001	3.78	54	−20	−24
Inferior frontal gyrus, triangular part/insula	R	29	<.001	3.74	36	24	10
Supramarginal gyrus/postcentral gyrus	R	8	<.001	3.68	52	−30	44
Postcentral gyrus	R	9	<.001	3.65	42	−30	64
Superior parietal gyrus	R	9	.001	3.63	30	−48	48
Postcentral gyrus	R	7	.001	3.61	58	−20	32
Superior temporal gyrus	L	6	.001	3.56	−60	−20	10
Superior temporal gyrus	R	5	.001	3.52	46	−36	12
Inferior frontal gyrus, triangular part	R	8	.001	3.51	38	32	10

The peak MNI coordinates are reported. Anatomical labels were assigned from the AAL3 atlas (Rolls et al., 2020) using the xjView 10.0 toolbox (https://www.alivelearn.net/xjview). L = left hemisphere; R = right hemisphere.

Table 3. Brain Regions Showing Positive Associations between fMRI Responses to Predictable > Unpredictable Blocks and Statistical Knowledge Score of the Predictable Blocks

		Cluster Level	*Voxel Level*		*MNI Coordinates (mm)*		
Region		*Cluster Size*	*p(Uncorrected)*	*t Value*	*x*	*y*	*z*
Insula/Rolandic operculum	R	123	<.001	4.04	40	−12	10
Inferior parietal gyrus	R	13	<.001	3.96	52	−38	56
Pallidum/putamen	R	11	<.001	3.74	18	6	0
Supramarginal gyrus	R	14	<.001	3.69	60	−28	46
Inferior/middle frontal gyrus, triangular part	R	13	.001	3.63	40	36	6

The peak MNI coordinates are reported. Anatomical labels were assigned from the AAL3 atlas (Rolls et al., 2020) using the xjView 10.0 toolbox (https://www.alivelearn.net/xjview). L = left hemisphere; R = right hemisphere.

albeit these activation clusters were much less extensive. For the unpredictable than predictable blocks, significantly larger activity was found bilaterally in the precuneus. Furthermore, smaller activation clusters were significant in the right middle and left superior temporal gyrus (see Table 1 and Figure 3; the images in Figure 3 are displayed with a cluster extent of ≥ 20).

Regression Analyses

Overall performance. This whole-brain multiple regression analysis examined which brain regions showed positive associations between fMRI responses in the predictable blocks (predictable > unpredictable) and overall performance score. It showed that larger activity in the predictable than in the unpredictable blocks mostly in the (1) bilateral insula extending to the Rolandic operculum and the superior temporal gyrus, in the (2) left superior/middle temporal gyrus, in the (3) right supramarginal gyrus, and in the (4) right inferior frontal gyrus was related to a higher overall performance score at the behavioral level (see Table 2 and Figure 4 for these and further clusters; the images in Figure 4 are displayed with a cluster extent of ≥ 20).

Statistical knowledge in the predictable blocks. This regression examined which brain regions showed positive associations between fMRI responses in the predictable

Table 4. Brain Regions Showing Positive Associations between fMRI Responses and Statistical Knowledge Score of the Unpredictable Blocks

		Cluster Level	*Voxel Level*		*MNI Coordinates (mm)*		
Region		*Cluster Size*	*p(Uncorrected)*	*t Value*	*x*	*y*	*z*
Predictable > unpredictable							
Middle/inferior frontal gyrus, triangular part	R	32	<.001	4.26	38	40	4
Hippocampus	R	6	<.001	3.87	32	−22	−8
Superior parietal gyrus/postcentral gyrus/precuneus	R	12	<.001	3.82	16	−54	72
Insula	L	10	<.001	3.73	−32	24	6
Insula	R	11	<.001	3.69	48	−2	2
Unpredictable > predictable							
Undefined/white matter	R	7	.001	3.55	26	−54	16
Unpredictable > rest							
Angular gyrus	L	32	<.001	4.16	−36	−66	38
Superior/middle frontal gyrus	L	13	<.001	3.88	−22	28	58
Angular gyrus	R	13	<.001	3.88	42	−72	38

The peak MNI coordinates are reported. Anatomical labels were assigned from the AAL3 atlas (Rolls et al., 2020) using the xjView 10.0 toolbox (https://www.alivelearn.net/xjview). L = left hemisphere; R = right hemisphere.

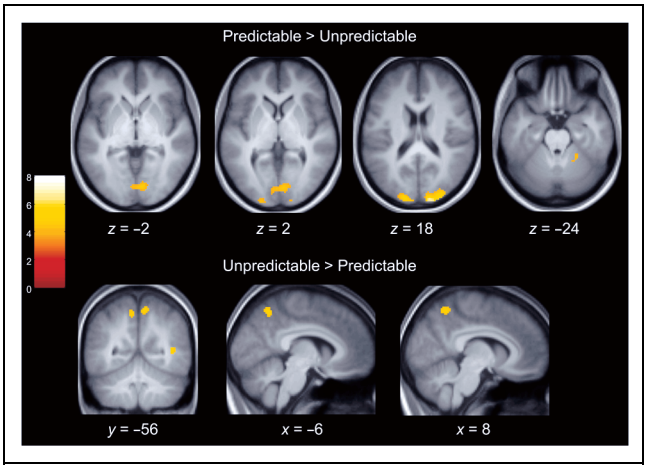

Figure 3. Results of the whole-brain, random-effects analysis of block predictability. Upper row: Activation clusters are presented for the predictable > unpredictable contrast (bilateral cuneus/superior occipital gyrus [$z = 18$], right lingual gyrus [$z = -2$], and right anterior cerebellum [$z = -24$]). Lower row: Activation clusters are presented for the unpredictable > predictable contrast (bilateral precuneus [$x = -6, x = 8, y = -56$] and right middle temporal gyrus [$y = -56$]). Statistical maps displayed on axial, sagittal, and coronal slices of the mean normalized structural image of all participants are FDR-corrected at voxel level ($p < .050$) with a cluster extent of ≥ 20. The color bar represents t values. MNI coordinates in mm are indicated below each slice.

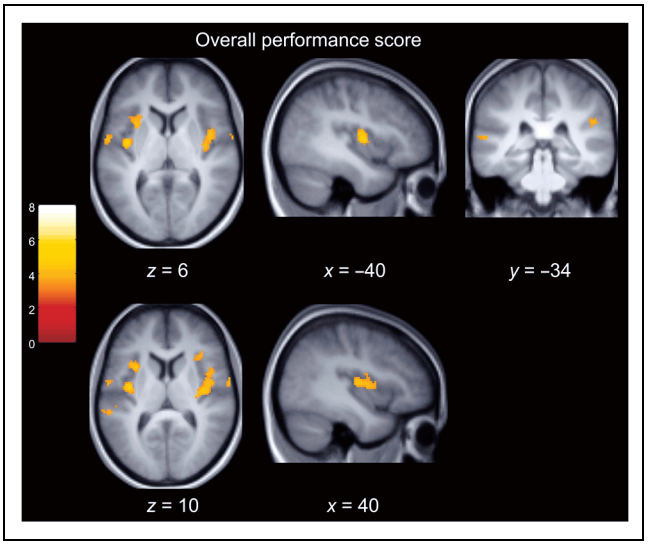

Figure 4. Results of the whole-brain, random-effects multiple regression analyses: overall performance score. Activation clusters showing positive associations between the predictable > unpredictable contrast and overall performance score are presented (bilateral insular activity [$x = -40, x = 40$] extending to the superior temporal gyrus and right inferior frontal gyrus [$z = 6, z = 10$], right supramarginal gyrus, and left superior temporal gyrus [$y = -34$]). Statistical maps displayed on axial, sagittal, and coronal slices of the mean normalized structural image of all participants are uncorrected at voxel level ($p \leq .001$) with a cluster extent of ≥ 20. The color bar represents t values. MNI coordinates in mm are indicated below each slice.

blocks (predictable > unpredictable) and overall statistical knowledge score of the same blocks. It showed that larger activity in the predictable than in the unpredictable blocks in the (1) insula extending to the Rolandic operculum, in the (2) inferior parietal gyrus, in the (3) globus pallidus/putamen, in the (4) supramarginal gyrus, and in the (5) inferior frontal gyrus was related to higher statistical knowledge score in the predictable blocks (see Table 3 and Figure 5). These brain activations appeared only in the right hemisphere. Thus, larger activity in these regions in the predictable blocks was associated with better triplet learning at the behavioral level, when triplet probabilities were indeed biased.

Statistical knowledge in the unpredictable blocks. As described in the Behavioral Results section, unpredictable triplets were processed similarly to the predictable ones, albeit the statistical knowledge score was attenuated. In support of this finding, statistical knowledge scores of the two block types were moderately correlated, $r = .595, p = .001$. Therefore, this group of regressions examined the generalization and persistence of the acquired statistical knowledge across the block types. First, positive associations between the predictable > unpredictable contrast and overall statistical knowledge score of the unpredictable blocks were tested. Larger activity in the predictable than in the unpredictable blocks in the (1) right middle/inferior frontal gyrus, in the (2) right hippocampus, in the (3) right superior parietal gyrus, as well as in the (4) bilateral insula was related to higher statistical knowledge score in the unpredictable blocks (see Table 4 and Figure 6). Thus, larger activity in these regions in the predictable blocks was associated with better triplet learning at the behavioral level, when triplet probabilities were in fact equal. Second, the regression analysis involving the opposite fMRI contrast (unpredictable > predictable) yielded a small cluster of activation in an undefined

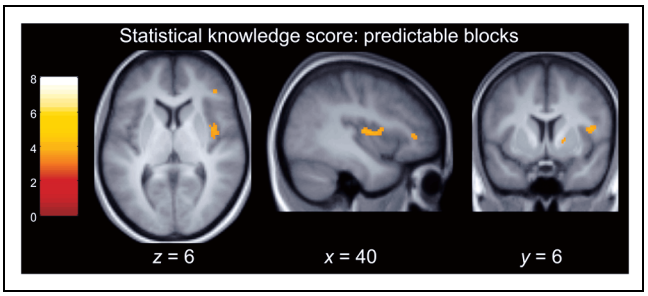

Figure 5. Results of the whole-brain, random-effects multiple regression analyses: statistical knowledge in the predictable blocks. Activation clusters showing positive associations between the predictable > unpredictable contrast and statistical knowledge score of the predictable blocks are presented (right insula and inferior frontal gyrus [$z = 6, x = 40$], right globus pallidus/putamen [$y = 6$]). Statistical maps displayed on axial, sagittal, and coronal slices of the mean normalized structural image of all participants are uncorrected at voxel level ($p \leq .001$) with a cluster extent of ≥ 5. The color bar represents t values. MNI coordinates in mm are indicated below each slice.

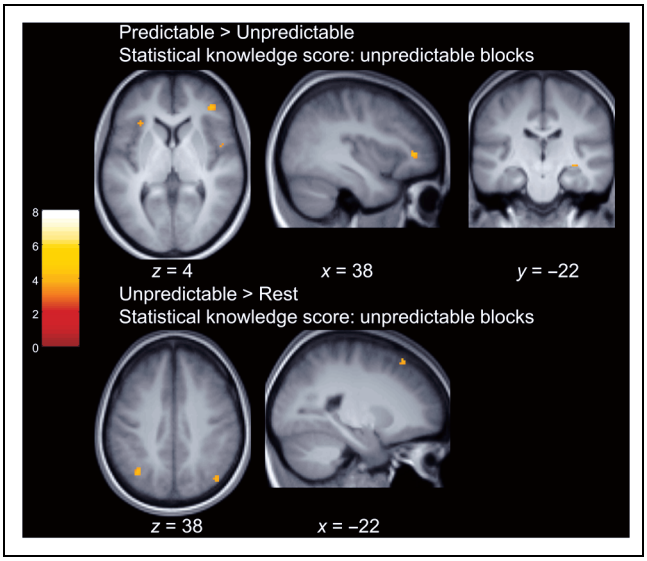

Figure 6. Results of the whole-brain, random-effects multiple regression analyses: statistical knowledge in the unpredictable blocks. Upper row: Activation clusters showing positive associations between the predictable > unpredictable contrast and statistical knowledge score of the unpredictable blocks are presented (bilateral insula and right inferior frontal gyrus [$z = 4, x = 38$], right hippocampus [$y = -22$]). Lower row: Activation clusters showing positive associations between the unpredictable > rest contrast and statistical knowledge score of the unpredictable blocks are presented (bilateral angular gyrus [$z = 38$], left superior/middle frontal gyrus [$x = -22$]). Statistical maps displayed on axial, sagittal, and coronal slices of the mean normalized structural image of all participants are uncorrected at voxel level ($p \leq .001$) with a cluster extent of ≥ 5. The color bar represents t values. MNI coordinates in mm are indicated below each slice.

right temporal area within the white matter (see Table 4). This result suggests that brain activity specific to the unpredictable blocks was not related to the magnitude of the statistical knowledge score at the behavioral level in the same blocks. Third, the regression analysis involving the unpredictable > rest contrast showed that larger activity in the unpredictable blocks in the (1) bilateral angular gyrus and in the (2) left superior/middle frontal gyrus was related to higher statistical knowledge score in the same blocks (see Table 4 and Figure 6).

In summary, brain activity specific to the predictable blocks supported not only the acquisition of statistical knowledge but also the transmission of this knowledge from the predictable to the unpredictable blocks, albeit relying on partly different brain regions. Larger activities of the right/bilateral insula and the right inferior frontal gyrus were related to increased statistical knowledge in both block types. However, distinct associations were also revealed: Although activity of the right globus pallidus/putamen was associated with increased statistical knowledge in the predictable blocks, activity of the right hippocampus was associated with that of the unpredictable blocks. Because brain activity specific to the unpredictable blocks was not related to statistical knowledge score in the same blocks, we could not identify brain regions uniquely contributing to the persistence of statistical knowledge in the unpredictable blocks. Yet, when neurocognitive processes related to task performance during the unpredictable blocks were considered (as opposed to the rest periods), activity of the bilateral angular gyrus and that of the left superior/middle frontal gyrus were associated with increased statistical knowledge in the unpredictable blocks.

DISCUSSION

Summary of Results

We examined the neural correlates of the implicit acquisition of statistical regularities as well as the persistence of the acquired representations using fMRI. We found significant learning of statistical regularities in the predictable blocks. Moreover, during the second half of the task, stimuli appearing with equal probability in the unpredictable blocks were also responded to according to the statistical knowledge acquired and established in the predictable blocks. However, the extent of statistical knowledge was greater when the distribution of statistical regularities was indeed biased. These behavioral results imply that knowledge of the biased probability structure is generalized to subsequent unpredictable stimuli; however, this knowledge is also influenced by the block-wise changes in stimulus predictability.

The larger brain activity for predictable than unpredictable blocks appeared to be the most widespread in the early visual cortex bilaterally. Meanwhile, when examining the associations between predictability-dependent brain activity (predictable vs. unpredictable blocks) and behavioral measures, larger activities of the bilateral insula and the right inferior frontal gyrus were related to better overall performance and increased statistical knowledge in both block types. Different associations between brain activity specific to the predictable blocks and statistical knowledge in the predictable and unpredictable blocks were also found. In addition to the other brain areas, these indicate the role of the right globus pallidus/putamen in the emergence of statistical knowledge and the role of the right hippocampus in the transmission of this knowledge from predictable to unpredictable blocks. However, brain areas uniquely contributing to the persistence of statistical knowledge were not identified because brain activity specific to the unpredictable blocks was unrelated to statistical knowledge in the same blocks. Still, the persistence of statistical knowledge was evidenced by activities of the bilateral angular gyrus and the left superior/middle frontal gyrus emerging during task performance in the unpredictable blocks.

Interpretation of Behavioral Results

Overall, the responses were slower and less accurate in the unpredictable than in the predictable blocks, indicating

sensitivity and adaptation to the changes in stimulus predictability. Statistical regularities were acquired in the predictable blocks, and this knowledge was further applied in the unpredictable blocks. These behavioral results are consistent with our previous study and extend beyond it. In the earlier study, the predictability of task blocks changed only once, in the middle of the paradigm (Kóbor et al., 2020). Here, participants were not exposed to the predictable blocks for an extended period because the underlying regularity determining stimulus presentation changed in every minute. Under these circumstances, acquisition of statistical regularities was still observed, irrespective of their actual probability. Although persistent implicit knowledge of statistical regularities has been evidenced in similar tasks at the behavioral level (Kóbor et al., 2017; Bulgarelli & Weiss, 2016; Nemeth & Janacsek, 2011; Romano, Howard, & Howard, 2010; Gebhart, Aslin, & Newport, 2009), our results suggest persistence even if statistical regularities dynamically change and become unpredictable multiple times over the paradigm.

The magnitude of the statistical knowledge score in this study was comparable to that of Kóbor and colleagues (2020). In both studies, the temporal characteristics of the task were the same and the sample characteristics were similar, which probably contributed to the observed effects. In fact, there are several factors modulating the magnitude of the statistical knowledge score, for instance, the temporal characteristics of stimulus presentation, the acquisition of statistical regularities (incidental or intentional), the type of the underlying sequence (deterministic or probabilistic), and the characteristics of the sample (e.g., age and clinical status of participants). These factors are detailed next.

First, in self-paced ASRT tasks with fast stimulus presentation rate, higher statistical knowledge scores (ca. 10–15 msec) have been observed (Kóbor et al., 2017; Stark-Inbar, Raza, Taylor, & Ivry, 2017; Nemeth et al., 2010). In fixed-paced tasks (Kóbor et al., 2020, 2021; Tóth et al., 2017), such as the present one, and in those with slow stimulus presentation rate (Kiss, Nemeth, & Janacsek, 2022; Kóbor et al., 2019, 2021), reduced statistical knowledge scores (ca. 5–10 msec) have been found. However, these were still robust and characterized by large effect sizes. Considering the time-on-task effects, statistical knowledge scores usually increased as the task progressed, irrespective of the temporal characteristics of the task. Second, statistical knowledge score could be lower if acquisition is incidental, such as in the present study, and higher if acquisition is intentional because of experimental manipulation (Nemeth, Janacsek, & Fiser, 2013). Third, the acquisition of probabilistic sequences as opposed to deterministic ones is expected to reduce the statistical knowledge score. In deterministic sequences, the consecutive sequence elements can be predicted from the previous ones with 100% certainty. Meanwhile, in probabilistic sequences, the predictability of a given element is less than 100%, leading to uncertain, more difficult predictions (Maheu, Meyniel, & Dehaene, 2022; Conway, 2020; Janacsek & Nemeth, 2012; Howard & Howard, 1997). This uncertainty can be coupled with reduced statistical knowledge. Finally, our young adult participants responded quickly from the outset of the task. They became faster until the second half of the task; however, their response speed no longer changed thereafter (see the Behavioral Results section). Hence, it is possible that less room remained for further RT improvements throughout the task, resulting in an inherently attenuated statistical knowledge score that is also related to RT differences (to high- vs. low-probability triplets).

In summary, these four factors (fixed-paced design, probabilistic sequence, implicit and incidental acquisition, and young adult participants with fast RTs) might have jointly reduced the magnitude of statistical knowledge, or at least its momentary expression reflected by the statistical knowledge score (see Kiss et al., 2022). Nevertheless, in the current study, the statistical knowledge score of the predictable blocks coupled with the triplet main effect (i.e., faster RTs to high- than to low-probability triplets) characterized by a large effect size can be interpreted as reflecting robust statistical knowledge that was generalized to the unpredictable blocks. We should also consider the ecological value of these behavioral findings and their relevance to real-world settings such as skill acquisition or language learning. It is important to bear in mind that these real-world acquisition processes involve extended periods of practice and refinement within a continuous cycle of regularity extraction, consolidation, and rewiring. Even implicit statistical learning itself is a slow, gradual process, with peak performance only attained after extended practice (Conway, 2020; Henke, 2010; Cleeremans, Destrebecqz, & Boyer, 1998). Our experiment cannot fully capture the complexity and emergence of real-world acquisition processes; however, it can provide insight into how these processes evolve. As such, even small differences in magnitude can be amplified into much more pronounced effects in the long run and can potentially be consequential and interpretable over time (Götz, Gosling, & Rentfrow, 2022; Funder & Ozer, 2019). Therefore, the findings regarding statistical knowledge, although small in absolute terms, can help us understand how environmental regularities are extracted and acquired.

It is conceivable that task characteristics contributed to the persistence of this statistical knowledge that was not consciously accessible based on the posttask questionnaire (cf. Vékony et al., 2022). Particularly, the acquisition of statistical information occurred in an implicit and incidental manner in a perceptually stable learning environment where participants were not instructed to monitor changes in the task structure (Kóbor et al., 2020). Thus, in the unpredictable blocks, participants probably followed the already established implicit representations of the triplet-level structure when processing the forthcoming stimuli, irrespective of their actual predictability. The slowing of responses in the unpredictable blocks as

compared with the predictable ones might not have been a noticeable block-to-block performance drop from the participants' viewpoint. Indeed, participants became faster and more accurate over the task, irrespective of block type. Consequently, response slowing in the unpredictable blocks can be regarded as a reasonable and economic strategy for adapting to the changed predictability of statistical regularities.

Importantly, however, statistical knowledge influenced the responses to a lesser extent in the unpredictable blocks. In terms of effect size measures, statistical knowledge in the unpredictable blocks was only 40% of that of the predictable blocks. Crucially, the difference in statistical knowledge between the block types was significant and appeared with a large effect size. This might suggest that although knowledge of the predictable structure influenced responding to unpredictable stimuli, this knowledge was not generalized and used unconditionally throughout the task. Previously, the presentation of different predictable statistical structures in smaller alternating blocks and the inhibition of overlearning the primary structure facilitated the simultaneous learning of the new structure (Bulgarelli & Weiss, 2016; Zinszer & Weiss, 2013). Although we investigated transitions between biased and equal probabilities instead of transitions between different statistical structures, the rapidly varying presentation of predictable and unpredictable blocks still attenuated the influence of biased probabilities (cf. Rey et al., 2020). As described in the next section, the fMRI results, at least in part, suggest the detection of change in stimulus predictability beyond the overarching effect of biased triplet probabilities.

Interpretation of fMRI Results

Early Visual Cortex

The brain activity difference in the early visual cortex supported the differential stimulus processing in the predictable and unpredictable blocks. This activity is consistent with the findings of two previous studies (Rosenthal, Mallik, Caballero-Gaudes, Sereno, & Soto, 2018; Rosenthal, Andrews, Antoniades, Kennard, & Soto, 2016). The primary visual cortex as part of a larger processing network involving the hippocampus and the basal ganglia (Rosenthal et al., 2016) or the precuneus (Rosenthal et al., 2018) was found to support the implicit acquisition of deterministic sequences. In the present study, the larger activity for the predictable than the unpredictable blocks in the early visual cortex might imply that the actual predictability of statistical regularities was encoded. This suggests that not only feedforward input but also high-level abstract information could be represented in this brain area (Vetter et al., 2020; Chong, Familiar, & Shim, 2016; Petro & Muckli, 2016; Vetter, Smith, & Muckli, 2014; Smith & Muckli, 2010). Our results together with the previous findings (Rosenthal et al., 2016, 2018) show that the implicit acquisition of statistical regularities can be detected already at the early stages of visual cortical processing. Because participants could freely move their gaze during task solving, it is also plausible that anticipatory eye movements contributed to predictability-dependent brain activity differences in the early visual cortex. Learning-dependent anticipations have been found to be sensitive indicators of statistical learning (Zolnai et al., 2022; Vakil, Schwizer Ashkenazi, Nevet-Perez, & Hassin-Baer, 2021; Vakil, Bloch, & Cohen, 2017), which can be examined in future studies combining fMRI and eye-tracking.

Cerebellum

Predictability-dependent activation difference was also found in the right anterior cerebellum (Lobules IV-V). The cerebellum has been implicated in the acquisition, prediction, and anticipation of temporally and/or spatially structured sequences of movements and various events (Ma et al., 2021; Breska & Ivry, 2020; Van Overwalle et al., 2020; Leggio & Molinari, 2015; Ito, 2008; Hikosaka, Nakamura, Sakai, & Nakahara, 2002; Ivry & Keele, 1989). However, Lobules IV-V are parts of the anterior cerebellum, which is involved mostly in sensorimotor processing according to neuroimaging, clinical, and neuroanatomical evidence (e.g., Stoodley & Schmahmann, 2018; Bernard & Seidler, 2013; Stoodley & Schmahmann, 2009). In particular, hand movements are represented in Lobules IV-V (Stoodley & Schmahmann, 2016), which were essential in solving the present task. Thus, the activity we observed in the right anterior cerebellum most likely reflects the better detection and sensorimotor processing of predictable stimuli (cf. the activation cluster in the postcentral gyrus), which aids in the acquisition of statistical regularities per se. In line with this reasoning, right anterior cerebellar activity was found in the initial learning phase of an SRT task (Magon et al., 2020), where the perceptuomotor task demands could have been more challenging than in the later phases. Furthermore, a specific part of the anterior cerebellum, the vermis region of Lobule V, emerged in association with implicit sequence learning in an activation likelihood estimation meta-analysis (Bernard & Seidler, 2013). However, it seems that activity in the posterior, "cognitive" regions of the cerebellum during the SRT task should be interpreted as executive or attention-related functions contributing to sequence learning (Janacsek et al., 2020; Magon et al., 2020). The implicit nature of our task and the incidental acquisition of statistical regularities may explain why we found only limited posterior cerebellar activation in the vermis region of Lobule VI.

Precuneus

The activity was larger for the unpredictable than predictable blocks in the bilateral precuneus. The precuneus has been considered as an anatomically and functionally

heterogeneous multimodal hub region that connects to other parietal and prefrontal areas as well as to the superior temporal sulcus and subcortical structures; therefore, it is part of multiple functional networks and involved in high-level cognitive processes (van den Heuvel & Sporns, 2013; Margulies et al., 2009; Cavanna & Trimble, 2006). In SRT-like tasks, activity in the left posterior parietal cortex including the precuneus increased with decreasing stimulus predictability, that is, when stimuli were presented in a random order after following a deterministic or a probabilistic regularity (Bischoff-Grethe et al., 2001). Similarly, the processing of random versus predictable stimuli was related to larger precuneus activity either in the initial and final learning phases (Magon et al., 2020) or during the full length of learning (Rosenthal et al., 2018; Landau & D'Esposito, 2006). In line with these studies, we also found increased activity for the unpredictable blocks in the left and right precuneus.

This precuneus activity might reflect an error signal such that the equal probability structure of the unpredictable blocks deviated from the biased statistical regularities of the predictable blocks. In a previous study using linguistic stimuli, the posterior division of the precuneus, together with the posterior cingulate cortex, were sensitive to an unsignaled transition from one statistical structure to another structure (Karuza et al., 2016). Lower activity in these areas during the processing of the first structure resulted in less sensitivity to the change in structure and lower performance on the second structure. In the present study, it is conceivable that the change in stimulus predictability was implicitly detected. This might have led to the incomplete generalization of statistical knowledge at the behavioral level. At the same time, this brain activity modulation might have supported only the limited update of the same statistical knowledge.

Insula

Regression analyses using the predictable > unpredictable contrast showed that activation of the bilateral insula was associated with increased overall performance, and specifically with increased statistical knowledge in the predictable and unpredictable blocks, with more localized or unilateral (right-sided) activation in the latter cases. Previous literature reported inconclusive results in terms of insular activity. Better extraction of statistical regularities was related to increased insular activity in the SRT task (Hung et al., 2019; Rieckmann et al., 2010; Grafton, Hazeltine, & Ivry, 1995). However, decreased activation of the bilateral insula was also observed for sequenced stimuli as compared with random ones, which was explained as a type of a repetition suppression effect (Thomas et al., 2004). Furthermore, the insula was activated when artificial grammar sequences were acquired both implicitly and explicitly (Yang & Li, 2012). Altogether, there are numerous examples of insular activation in similar tasks, but its specific functional role in the current experiment requires further explanation and is described below.

In general, the mid-posterior portion of the insula can be functionally related to sensorimotor processing whereas the dorsal anterior portion can be related to cognitive processing (Kurth, Zilles, Fox, Laird, & Eickhoff, 2010). This division is supported by the connections of the mid-posterior portion with other brain regions for sensorimotor processing and that of the dorsal anterior portion with frontal, anterior cingulate, and parietal regions (Uddin, Nomi, Hébert-Seropian, Ghaziri, & Boucher, 2017). In the present study, activation clusters covered both the mid-posterior and the dorsal anterior portions of the insula. Our regressions further revealed increased activations in the inferior/middle frontal gyrus, postcentral gyrus, supramarginal gyrus, superior/inferior parietal gyrus, and superior temporal gyrus coupled with increased overall performance and statistical knowledge. Activity in these areas might have been connected to the observed insular activity. However, this hypothesis should be tested with additional connectivity analyses. Finding actual connections between these areas would indicate that the insula contributes to both sensorimotor and cognitive processing in the present task.

Information from the different functional domains of the insula seems to be integrated in its dorsal anterior portion to maintain task performance (Kurth et al., 2010). This functional integration would be critical in our rapid visuomotor task with hidden and changing probability structure to ensure efficient task solving. Similarly, salience processing and novelty detection have also been recognized as key functions of the (dorsal anterior) insula (Uddin et al., 2017; Uddin, 2015). Statistical knowledge is based on the differentiation of high- versus low-probability triplets, which manifests mainly in the speeding up of RTs to high-probability triplets. Although high-probability triplets are frequent by their very nature in the predictable blocks, their relevance in acquiring the hidden probability structure to achieve high task performance would still make them "salient." The enhanced insular activation, therefore, can be explained as reflecting salience processing in terms of the predictable statistical regularities. Because of the transmission of statistical knowledge across the block types, this could also apply to the high-probability triplets of the unpredictable blocks where they are no longer frequent.

Inferior Frontal Gyrus

Regression analyses using the predictable > unpredictable contrast also revealed that the activity of the right inferior frontal gyrus was associated with better overall performance and increased statistical knowledge in both block types. The overlapping activity between the two block types was found in the triangular part of the right inferior frontal gyrus. Previous studies showed that the left inferior frontal gyrus has been involved in the processing of

statistical and sequential information in different modalities (Batterink et al., 2019; Frost, Armstrong, Siegelman, & Christiansen, 2015). In an EEG study using a source localization method, the right inferior frontal gyrus was specifically implicated in the acquisition of visual statistical regularities embedded in a variant of the ASRT task (Takács et al., 2021). This aligns with those results showing that the right inferior frontal gyrus is not specific to inhibitory control functions but supports the detection of novelty and frequency information (Erika-Florence, Leech, & Hampshire, 2014). In our study, this role of the right inferior frontal gyrus could be reflected by the increased overall performance and the increased statistical knowledge in the predictable blocks. Although behavioral responses in the unpredictable blocks were adjusted to the biased probabilities of the predictable blocks, the right inferior frontal gyrus activity specific to the predictable blocks could also mirror the changed frequency of these probabilities. However, the latter assumption should be tested in further studies. Altogether, the observed activity of the right inferior frontal gyrus not only corroborates previous research but also indicates the sensitivity of this area to the presence of statistical regularities, even if their true distribution changes.

Globus Pallidus/Putamen versus Hippocampus

Beyond the common regions, regression analyses using the predictable > unpredictable contrast revealed unique associations between brain activity in the predictable blocks and statistical knowledge in the predictable versus unpredictable blocks. The right globus pallidus/putamen activity was related to statistical knowledge in the predictable blocks. In contrast, the right hippocampal activity was related to statistical knowledge in the unpredictable blocks. Activity of the right globus pallidus/putamen supports the basal ganglia-based processing of the predictable structure, in line with several studies using the SRT task and other paradigms measuring implicit sequence or statistical learning (Conway, 2020; Janacsek et al., 2020; Batterink et al., 2019). The insular activity appearing in relation to overall performance (see Table 2) also extended to the right putamen to a small extent. These converging findings might imply that the differentiation of predictable and unpredictable blocks is rooted in the processing of biased triplet probabilities, supported by the right globus pallidus/putamen.

Increased (right) hippocampal activity in the predictable blocks was related to increased statistical knowledge only in the unpredictable blocks and not in the predictable ones, contrary to our expectations. Importantly, the hippocampus was not generally sensitive to the predictability of statistical regularities (i.e., the differentiation of block types), its activity emerged only in association with statistical knowledge measured at the behavioral level. These findings suggest that the hippocampus might not support the mere acquisition of statistical regularities but the transmission of statistical knowledge across the perceptually similar blocks (Zeithamova & Bowman, 2020; Albouy et al., 2013; Ross et al., 2009; Shohamy & Wagner, 2008).

It seems that applying one kind of statistical knowledge throughout the task was an effective strategy (see the Interpretation of Behavioral Results section above). When statistical knowledge acquired in the predictable blocks was relevant, the globus pallidus/putamen activity supported the exploitation of this knowledge (Albouy et al., 2013). Because no learnable stimulus dependencies were present in the unpredictable blocks, it is possible that participants stuck to the more viable representations of biased probabilities. The hippocampus might have supported this strategy by maintaining the representations of biased statistical regularities even when the statistical knowledge was irrelevant because of the equal probability structure.

These specific, statistical learning–dependent activations appeared primarily in the right hemisphere. The prominent role of the right hemisphere in statistical learning has been shown in meta-analyses involving similar visuomotor SRT tasks (Janacsek et al., 2020; Hardwick et al., 2013), in studies using non-invasive brain stimulation (Janacsek, Ambrus, Paulus, Antal, & Nemeth, 2015; Galea, Albert, Ditye, & Miall, 2010), as well as in the case of split-brain, frontal lobe-lesioned (Roser, Fiser, Aslin, & Gazzaniga, 2011; Wolford, Miller, & Gazzaniga, 2000), and right-brain-damaged patients (Danckert, Stöttinger, Quehl, & Anderson, 2012). However, in auditory statistical learning tasks, increased activity in higher level auditory regions, such as the left superior temporal gyrus and the left inferior frontal gyrus, was found (for reviews, see Batterink et al., 2019; Frost et al., 2015). Therefore, hemispheric differences could be specific to the content and modality of the task used for measuring statistical learning.

Angular Gyrus

Regression analysis using the unpredictable > rest contrast showed that larger activity of the bilateral angular gyrus during task performance in the unpredictable blocks was related to increased statistical knowledge in the same blocks. This can be considered as further evidence for the generalization of statistical knowledge. The angular gyrus has been regarded as a multisensory, cross-modal association and integration area that plays a role in a wide range of cognitive operations (Seghier, 2013). For instance, it has been suggested that the angular gyrus extracts the spatiotemporally extended sequential structure of events through experience. This contributes to episodic retrieval and enables the integration of episodic and semantic memories (Humphreys, Lambon Ralph, & Simons, 2021). Furthermore, representations of rule-based associations and low-level visual features related to consolidated schema memories converged within the left angular gyrus during retrieval (Wagner et al., 2015). The left angular

gyrus also supported the recognition of acquired statistical regularities after being exposed to them in an auditory statistical learning task (Ordin, Polyanskaya, & Soto, 2020). On the basis of these results, it is conceivable that the predominantly left-sided activity of the angular gyrus we found here is also related to the retrieval of statistical knowledge. However, the present task did not reveal any consciously accessible statistical knowledge, and the binding of different pieces of information was not critical, in contrast to the referred studies. Therefore, any speculation regarding the retrieval of statistical knowledge in this case should be approached with caution.

Meanwhile, this finding may be related to a recent study that showed consistent modulation of the left angular gyrus and its functional connections through implicit statistical learning (Park et al., 2022). The regression performed here also revealed activity of the left superior/middle frontal gyrus that is structurally connected to the angular gyrus (Seghier, 2013). Again, in the study of Park and colleagues (2022), during statistical learning, the left superior frontal gyrus had strong negative functional connections with the salience, language, and dorsal attention networks, similarly to the left angular gyrus. Our study did not examine the connectivity between these areas and other brain regions or networks, and we found these activities only during performance in the unpredictable blocks. However, despite any reservations, it appears that both the left angular and superior frontal gyri may be involved not only in the acquisition but also in the retrieval and application of implicit statistical knowledge.

Rest periods were used as the baseline in the unpredictable > rest contrast, which can introduce the problem of individual variability (Ordin et al., 2020). In particular, rest periods are characterized by different cognitive processes involving various brain networks (Gonzalez-Castillo et al., 2019). These cognitive processes can vary significantly across individuals, contributing differently to brain activity during rest. Furthermore, the fMRI responses, as well as motion and arousal, can also vary individually and may not be typical for the given experimental condition (i.e., unpredictable blocks) unless compared with another active condition. Therefore, although the results of the regression using the unpredictable > rest contrast appear reasonable and unbiased, it is important to acknowledge the related methodological limitations.

The Generalization and Persistence of Statistical Knowledge

At the behavioral level, the difference in statistical knowledge between predictable and unpredictable blocks suggests incomplete generalization or partial updating because of exposure to the equal probability structure. The fMRI results imply the clear differentiation of predictable and unpredictable blocks. However, according to the regression analyses, there are multiple pieces of evidence that indicate generalization at the brain level. Regarding brain activity specific to the predictable blocks, it is likely that the right insula, inferior frontal gyrus, and hippocampus support the transmission and preservation of statistical knowledge. During task performance in the unpredictable blocks, activity in the bilateral angular gyrus and the left superior/middle frontal gyrus might underpin the retrieval and application of statistical knowledge. The lack of associations between brain activity specific to the unpredictable blocks and statistical knowledge might be considered as evidence against the generalization and persistence of statistical knowledge. Nevertheless, the findings altogether more strongly suggest that statistical knowledge was generalized to and implicitly retrieved in an irrelevant context without a predictable structure.

Conclusions

Behavioral and fMRI results jointly indicate that even if the stimulus structure rapidly changes, humans build persistent representations of the predictable patterns. More importantly, when the actual predictable patterns are lacking, unpredictable stimuli are still processed according to these representations. The emergence of these representations partly depends on the right globus pallidus/putamen. The representations appear to be strengthened by the hippocampus, insula, and inferior frontal gyrus in the right hemisphere, as well as by the bilateral angular gyrus. Although the influence of the predictable patterns is attenuated in the unpredictable context, the update of the representations appears to be only partial. Altogether, during the implicit acquisition of predictable patterns, robust habit-like performance develops.

APPENDIX

Analysis of Accuracy Data

Overall Performance at the Level of Block Types

The Block Type × Run ANOVA on the accuracy data revealed significant main effects of Block Type, $F(1, 31) = 27.30$, $p < .001$, $\eta_p^2 = .468$, and Run, $F(7, 217) = 8.72$, $\varepsilon = .559$, $p < .001$, $\eta_p^2 = .220$, while their interaction was nonsignificant, $F(7, 217) = 0.66$, $\varepsilon = .675$, $p = .646$, $\eta_p^2 = .021$. The significant main effects indicate more accurate responding in the predictable than in the unpredictable blocks ($M = 85.4\%$, $SD = 8.1$ vs. $M = 84.2\%$, $SD = 8.6$) and an increase in response accuracy as the task progresses (from $\text{Run}_1 = 82.0\%$ to $\text{Run}_8 = 87.3\%$). As unpredictable stimuli deteriorated accurate responding, participants probably became sensitive to the changes of stimulus predictability. The next analysis investigates whether sensitivity to the biased triplet probabilities has emerged also at the level of accuracy.

Table A1. Mean Percentage (%) and Standard Deviation of Response Accuracy Split by Triplet Type and Block Type

	High-probability Triplets		*Low-probability Triplets*	
	M (*SD*)		*M* (*SD*)	
	Predictable	*Unpredictable*	*Predictable*	*Unpredictable*
Run_1	82.7 (9.5)	82.3 (13.7)	81.9 (9.7)	81.9 (10.2)
Run_2	85.9 (9.0)	85.0 (9.6)	83.6 (10.4)	82.9 (9.3)
Run_3	84.1 (10.3)	83.7 (12.2)	83.6 (10.2)	81.6 (10.3)
Run_4	85.8 (8.5)	83.5 (11.3)	83.3 (10.4)	83.1 (10.0)
Run_5	86.1 (8.8)	85.8 (10.3)	83.5 (9.0)	84.0 (9.0)
Run_6	86.5 (9.8)	86.6 (9.0)	84.7 (11.0)	84.8 (8.8)
Run_7	87.7 (7.1)	86.5 (8.3)	86.2 (7.0)	85.5 (9.0)
Run_8	88.8 (7.9)	88.0 (6.6)	88.0 (7.9)	87.1 (8.8)
Overall	85.9 (8.1)	85.2 (8.7)	84.3 (8.2)	83.9 (8.6)
Session 1	84.6 (8.7)	83.6 (10.2)	83.1 (9.0)	82.4 (9.2)
Session 2	87.3 (7.9)	86.7 (7.8)	85.6 (7.9)	85.3 (8.5)

Triplet Learning

The Block Type × Triplet × Run ANOVA revealed significant main effects of Block Type, $F(1, 31) = 8.99, p = .005$, $\eta_p^2 = .225$; Triplet, $F(1, 31) = 26.68, p < .001$, $\eta_p^2 = .463$; and Run, $F(7, 217) = 8.15, \varepsilon = .543, p < .001$, $\eta_p^2 = .208$. The two-way and three-way interactions of these factors were nonsignificant, Block Type × Triplet, $F(1, 31) = 0.45, p = .506$, $\eta_p^2 = .014$; Block Type × Run, $F(7, 217) = 0.53, \varepsilon = .671, p = .742$, $\eta_p^2 = .017$; Triplet × Run, $F(7, 217) = 0.75, \varepsilon = .725, p = .590$, $\eta_p^2 = .024$; Block Type × Triplet × Run, $F(7, 217) = 0.68, p = .686$, $\eta_p^2 = .022$. As in the earlier analysis, the significant main effect of Block Type revealed higher accuracy in the predictable than in the unpredictable blocks. On the basis of the pairwise comparisons related to the significant main effect of Run, accuracy was the highest in the last run (Run_8, 88.0%), differing significantly from all previous runs ($ps \leq .008$). Indeed, from Run_3, accuracy increased gradually until the end of the task, albeit not all pairwise differences were significant.

The significant Triplet main effect indicated higher accuracy to high-probability than to low-probability triplets ($M = 85.6\%$, $SD = 8.4$ vs. $M = 84.1\%$, $SD = 8.3$), irrespective of their actual predictability (i.e., considering block type). Thus, in line with the RT findings, participants responded according to their statistical knowledge emerging over the predictable blocks even when the biased distribution of triplets was absent in the unpredictable blocks. For the sake of completeness, response accuracy split by triplet type and block type in each run, averaged for the entire task as well as for the first ($Runs_{1–4}$) and second ($Runs_{5–8}$) scanning sessions, respectively, are provided in Table A1. For each triplet type, mean accuracy increased significantly from the first to the second session ($ps \leq .003$).

Acknowledgments

The authors thank the help of Eszter Somogyi and Dorottya Denke in fMRI and neuropsychological data acquisition.

Corresponding authors: Andrea Kóbor, Brain Imaging Centre, HUN-REN Research Centre for Natural Sciences, Magyar tudósok körútja 2., H–1117, Budapest, Hungary, or via e-mail: kobor.andrea@ttk.hu, or Dezso Nemeth, Centre de Recherche en Neurosciences de Lyon CRNL U1028 UMR5292, INSERM, CNRS, Université Claude Bernard Lyon 1, 95 Boulevard Pinel, F-69500 Bron, France, or via e-mail: dezso.nemeth@inserm.fr.

Data Availability Statement

Data supporting the findings of this study (processed behavioral data, first-level contrast images, second-level *t*-maps) are available via the Open Science Framework (https://osf.io/nx73e) in the ASRT_fMRI_data folder. Raw behavioral data and fMRI data in various formats (raw, preprocessed) will be provided from the corresponding author (A. K.) upon written request. No custom code was used to process the data described in the study. Standard functions of the SPM12 and the functional_art modular function of the CONN toolbox (as referred to in the main text) were applied for fMRI data analysis.

Author Contributions

Andrea Kóbor: Conceptualization; Data curation; Formal analysis; Funding acquisition; Methodology; Project

administration; Software; Visualization; Writing—Original draft. Karolina Janacsek: Conceptualization; Methodology; Software; Supervision; Writing—Review & editing. Petra Hermann: Data curation; Formal analysis; Resources; Software; Supervision; Writing—Original draft; Writing—Review & editing. Zsófia Zavecz: Conceptualization; Data curation; Investigation; Project administration; Writing—Review & editing. Vera Varga: Investigation; Project administration; Writing—Review & editing. Valéria Csépe: Supervision; Writing—Review & editing. Zoltán Vidnyánszky: Conceptualization; Funding acquisition; Project administration; Resources; Supervision; Writing—Review & editing. Gyula Kovács: Conceptualization; Methodology; Supervision; Writing—Review & editing. Dezso Nemeth: Conceptualization; Funding acquisition; Methodology; Supervision; Writing—Review & editing.

Funding Information

This research was supported by Project No. 124412 (PI: A. K.) and 124148 (PI: K. J.) that have been implemented with the support provided by the Ministry of Innovation and Technology of Hungary from the National Research, Development and Innovation Fund, financed under the FK and PD funding schemes, respectively. Furthermore, the research, A. K., and P. H. were supported by the National Brain Research Program by the Hungarian Academy of Sciences (project NAP2022-I-1/2022). The János Bolyai Research Scholarship of the Hungarian Academy of Sciences (to A. K. and K. J.) and the Chaire de Professeur Junior Program by INSERM and French National Research Agency (Chaire Inserm-ANR-22-CE64-001) (to D. N.) also supported this research.

Diversity in Citation Practices

Retrospective analysis of the citations in every article published in this journal from 2010 to 2021 reveals a persistent pattern of gender imbalance: Although the proportions of authorship teams (categorized by estimated gender identification of first author/last author) publishing in the *Journal of Cognitive Neuroscience (JoCN)* during this period were M(an)/M = .407, W(oman)/M = .32, M/W = .115, and W/W = .159, the comparable proportions for the articles that these authorship teams cited were M/M = .549, W/M = .257, M/W = .109, and W/W = .085 (Postle and Fulvio, *JoCN*, 34:1, pp. 1–3). Consequently, *JoCN* encourages all authors to consider gender balance explicitly when selecting which articles to cite and gives them the opportunity to report their article's gender citation balance.

REFERENCES

Albouy, G., Fogel, S., King, B. R., Laventure, S., Benali, H., Karni, A., et al. (2015). Maintaining vs. enhancing motor sequence memories: Respective roles of striatal and hippocampal systems. *Neuroimage*, *108*, 423–434. https://doi.org/10.1016/j.neuroimage.2014.12.049, PubMed: 25542533

Albouy, G., King, B. R., Maquet, P., & Doyon, J. (2013). Hippocampus and striatum: Dynamics and interaction during acquisition and sleep-related motor sequence memory consolidation. *Hippocampus*, *23*, 985–1004. https://doi.org/10.1002/hipo.22183, PubMed: 23929594

Albouy, G., Sterpenich, V., Balteau, E., Vandewalle, G., Desseilles, M., Dang-Vu, T., et al. (2008). Both the hippocampus and striatum are involved in consolidation of motor sequence memory. *Neuron*, *58*, 261–272. https://doi.org/10.1016/j.neuron.2008.02.008, PubMed: 18439410

Ances, B. M., Leontiev, O., Perthen, J. E., Liang, C., Lansing, A. E., & Buxton, R. B. (2008). Regional differences in the coupling of cerebral blood flow and oxygen metabolism changes in response to activation: Implications for BOLD-fMRI. *Neuroimage*, *39*, 1510–1521. https://doi.org/10.1016/j.neuroimage.2007.11.015, PubMed: 18164629

Aslin, R. N. (2017). Statistical learning: A powerful mechanism that operates by mere exposure. *Wiley Interdisciplinary Reviews: Cognitive Science*, *8*, e1373. https://doi.org/10.1002/wcs.1373, PubMed: 27906526

Bar, M. (2007). The proactive brain: Using analogies and associations to generate predictions. *Trends in Cognitive Sciences*, *11*, 280–289. https://doi.org/10.1016/j.tics.2007.05.005, PubMed: 17548232

Batterink, L. J., Paller, K. A., & Reber, P. J. (2019). Understanding the neural bases of implicit and statistical learning. *Topics in Cognitive Science*, *11*, 482–503. https://doi.org/10.1111/tops.12420, PubMed: 30942536

Bernard, J., & Seidler, R. (2013). Cerebellar contributions to visuomotor adaptation and motor sequence learning: An ALE meta-analysis. *Frontiers in Human Neuroscience*, *7*, 27. https://doi.org/10.3389/fnhum.2013.00027, PubMed: 23403800

Bischoff-Grethe, A., Martin, M., Mao, H., & Berns, G. S. (2001). The context of uncertainty modulates the subcortical response to predictability. *Journal of Cognitive Neuroscience*, *13*, 986–993. https://doi.org/10.1162/089892901753165881, PubMed: 11595100

Bönstrup, M., Iturrate, I., Thompson, R., Cruciani, G., Censor, N., & Cohen, L. G. (2019). A rapid form of offline consolidation in skill learning. *Current Biology*, *29*, 1346–1351. https://doi.org/10.1016/j.cub.2019.02.049, PubMed: 30930043

Brainard, D. H. (1997). The psychophysics toolbox. *Spatial Vision*, *10*, 433–436. https://doi.org/10.1163/156856897X00357, PubMed: 9176952

Breska, A., & Ivry, R. B. (2020). Context-specific control over the neural dynamics of temporal attention by the human cerebellum. *Science Advances*, *6*, eabb1141. https://doi.org/10.1126/sciadv.abb1141, PubMed: 33268365

Bubic, A., Von Cramon, D. Y., & Schubotz, R. (2010). Prediction, cognition and the brain. *Frontiers in Human Neuroscience*, *4*, 25. https://doi.org/10.3389/fnhum.2010.00025, PubMed: 20631856

Bulgarelli, F., & Weiss, D. J. (2016). Anchors aweigh: The impact of overlearning on entrenchment effects in statistical learning. *Journal of Experimental Psychology: Learning, Memory, and Cognition*, *42*, 1621–1631. https://doi.org/10.1037/xlm0000263, PubMed: 26950492

Cavanna, A. E., & Trimble, M. R. (2006). The precuneus: A review of its functional anatomy and behavioural correlates. *Brain*, *129*, 564–583. https://doi.org/10.1093/brain/awl004, PubMed: 16399806

Chong, E., Familiar, A. M., & Shim, W. M. (2016). Reconstructing representations of dynamic visual objects in early visual cortex. *Proceedings of the National Academy of Sciences, U.S.A.*, *113*, 1453. https://doi.org/10.1073/pnas.1512144113, PubMed: 26712004

Cleeremans, A., Destrebecqz, A., & Boyer, M. (1998). Implicit learning: News from the front. *Trends in Cognitive Sciences*, *2*, 406–416. https://doi.org/10.1016/S1364-6613(98)01232-7, PubMed: 21227256

Conway, C. M. (2020). How does the brain learn environmental structure? Ten core principles for understanding the neurocognitive mechanisms of statistical learning. *Neuroscience & Biobehavioral Reviews*, *112*, 279–299. https://doi.org/10.1016/j.neubiorev.2020.01.032, PubMed: 32018038

Danckert, J., Stöttinger, E., Quehl, N., & Anderson, B. (2012). Right hemisphere brain damage impairs strategy updating. *Cerebral Cortex*, *22*, 2745–2760. https://doi.org/10.1093/cercor/bhr351, PubMed: 22178711

Daselaar, S. M., Rombouts, S. A., Veltman, D. J., Raaijmakers, J. G., & Jonker, C. (2003). Similar network activated by young and old adults during the acquisition of a motor sequence. *Neurobiology of Aging*, *24*, 1013–1019. https://doi.org/10.1016/S0197-4580(03)00030-7, PubMed: 12928061

de Hollander, G., Keuken, M. C., & Forstmann, B. U. (2015). The subcortical cocktail problem; Mixed signals from the subthalamic nucleus and substantia nigra. *PLoS One*, *10*, e0120572. https://doi.org/10.1371/journal.pone.0120572, PubMed: 25793883

Dennis, N. A., & Cabeza, R. (2011). Age-related dedifferentiation of learning systems: An fMRI study of implicit and explicit learning. *Neurobiology of Aging*, *32*, 2318.e17–2318.e30. https://doi.org/10.1016/j.neurobiolaging.2010.04.004, PubMed: 20471139

Doyon, J., Bellec, P., Amsel, R., Penhune, V., Monchi, O., Carrier, J., et al. (2009). Contributions of the basal ganglia and functionally related brain structures to motor learning. *Behavioural Brain Research*, *199*, 61–75. https://doi.org/10.1016/j.bbr.2008.11.012, PubMed: 19061920

Dragovic, M. (2004a). Categorization and validation of handedness using latent class analysis. *Acta Neuropsychiatrica*, *16*, 212–218. https://doi.org/10.1111/j.0924-2708.2004.00087.x, PubMed: 26984309

Dragovic, M. (2004b). Towards an improved measure of the Edinburgh Handedness Inventory: A one-factor congeneric measurement model using confirmatory factor analysis. *Laterality: Asymmetries of Body, Brain and Cognition*, *9*, 411–419. https://doi.org/10.1080/13576500342000248, PubMed: 15513238

Du, Y., Prashad, S., Schoenbrun, I., & Clark, J. E. (2016). Probabilistic motor sequence yields greater offline and less online learning than fixed sequence. *Frontiers in Human Neuroscience*, *10*, 87. https://doi.org/10.3389/fnhum.2016.00087, PubMed: 26973502

Dutilh, G., Vandekerckhove, J., Forstmann, B. U., Keuleers, E., Brysbaert, M., & Wagenmakers, E.-J. (2012). Testing theories of post-error slowing. *Attention, Perception & Psychophysics*, *74*, 454–465. https://doi.org/10.3758/s13414-011-0243-2, PubMed: 22105857

Erika-Florence, M., Leech, R., & Hampshire, A. (2014). A functional network perspective on response inhibition and attentional control. *Nature Communications*, *5*, 4073. https://doi.org/10.1038/ncomms5073, PubMed: 24905116

Fletcher, P. C., Zafiris, O., Frith, C. D., Honey, R. A., Corlett, P. R., Zilles, K., et al. (2005). On the benefits of not trying: Brain activity and connectivity reflecting the interactions of explicit and implicit sequence learning. *Cerebral Cortex*, *15*, 1002–1015. https://doi.org/10.1093/cercor/bhh201, PubMed: 15537672

Forest, T. A., Schlichting, M. L., Duncan, K. D., & Finn, A. S. (2023). Changes in statistical learning across development. *Nature Reviews Psychology*, *2*, 205–219. https://doi.org/10.1038/s44159-023-00157-0

Friston, K. J., Williams, S., Howard, R., Frackowiak, R. S., & Turner, R. (1996). Movement-related effects in fMRI time-series. *Magnetic Resonance in Medicine*, *35*, 346–355. https://doi.org/10.1002/mrm.1910350312, PubMed: 8699946

Frost, R., Armstrong, B. C., & Christiansen, M. H. (2019). Statistical learning research: A critical review and possible new directions. *Psychological Bulletin*, *145*, 1128–1153. https://doi.org/10.1037/bul0000210, PubMed: 31580089

Frost, R., Armstrong, B. C., Siegelman, N., & Christiansen, M. H. (2015). Domain generality versus modality specificity: The paradox of statistical learning. *Trends in Cognitive Sciences*, *19*, 117–125. https://doi.org/10.1016/j.tics.2014.12.010, PubMed: 25631249

Funder, D. C., & Ozer, D. J. (2019). Evaluating effect size in psychological research: Sense and nonsense. *Advances in Methods and Practices in Psychological Science*, *2*, 156–168. https://doi.org/10.1177/2515245919847202

Galea, J. M., Albert, N. B., Ditye, T., & Miall, R. C. (2010). Disruption of the dorsolateral prefrontal cortex facilitates the consolidation of procedural skills. *Journal of Cognitive Neuroscience*, *22*, 1158–1164. https://doi.org/10.1162/jocn.2009.21259, PubMed: 19413472

Gebhart, A. L., Aslin, R. N., & Newport, E. L. (2009). Changing structures in midstream: Learning along the statistical garden path. *Cognitive Science*, *33*, 1087–1116. https://doi.org/10.1111/j.1551-6709.2009.01041.x, PubMed: 20574548

Gonzalez-Castillo, J., Caballero-Gaudes, C., Topolski, N., Handwerker, D. A., Pereira, F., & Bandettini, P. A. (2019). Imaging the spontaneous flow of thought: Distinct periods of cognition contribute to dynamic functional connectivity during rest. *Neuroimage*, *202*, 116129. https://doi.org/10.1016/j.neuroimage.2019.116129, PubMed: 31461679

Götz, F. M., Gosling, S. D., & Rentfrow, P. J. (2022). Small effects: The indispensable foundation for a cumulative psychological science. *Perspectives on Psychological Science*, *17*, 205–215. https://doi.org/10.1177/1745691620984483, PubMed: 34213378

Grafton, S. T., Hazeltine, E., & Ivry, R. (1995). Functional mapping of sequence learning in normal humans. *Journal of Cognitive Neuroscience*, *7*, 497–510. https://doi.org/10.1162/jocn.1995.7.4.497, PubMed: 23961907

Greenhouse, S. W., & Geisser, S. (1959). On methods in the analysis of profile data. *Psychometrika*, *24*, 95–112. https://doi.org/10.1007/bf02289823

Griswold, M. A., Jakob, P. M., Heidemann, R. M., Nittka, M., Jellus, V., Wang, J., et al. (2002). Generalized autocalibrating partially parallel acquisitions (GRAPPA). *Magnetic Resonance in Medicine*, *47*, 1202–1210. https://doi.org/10.1002/mrm.10171, PubMed: 12111967

Haak, K. V., & Beckmann, C. F. (2020). Understanding brain organisation in the face of functional heterogeneity and functional multiplicity. *Neuroimage*, *220*, 117061. https://doi.org/10.1016/j.neuroimage.2020.117061, PubMed: 32574808

Hardwick, R. M., Rottschy, C., Miall, R. C., & Eickhoff, S. B. (2013). A quantitative meta-analysis and review of motor learning in the human brain. *Neuroimage*, *67*, 283–297. https://doi.org/10.1016/j.neuroimage.2012.11.020, PubMed: 23194819

Henke, K. (2010). A model for memory systems based on processing modes rather than consciousness. *Nature Reviews Neuroscience*, *11*, 523–532. https://doi.org/10.1038/nrn2850, PubMed: 20531422

Hikosaka, O., Nakamura, K., Sakai, K., & Nakahara, H. (2002). Central mechanisms of motor skill learning. *Current Opinion in Neurobiology*, *12*, 217–222. https://doi.org/10.1016/S0959-4388(02)00307-0, PubMed: 12015240

Horváth, K., Kardos, Z., Takács, Á., Csépe, V., Nemeth, D., Janacsek, K., et al. (2021). Error processing during the online

retrieval of probabilistic sequence knowledge. *Journal of Psychophysiology*, *35*, 61–75. https://doi.org/10.1027/0269-8803/a000262
Horváth, K., Nemeth, D., & Janacsek, K. (2022). Inhibitory control hinders habit change. *Scientific Reports*, *12*, 8338. https://doi.org/10.1038/s41598-022-11971-6, PubMed: 35585209
Howard, J. H., Jr., & Howard, D. V. (1997). Age differences in implicit learning of higher order dependencies in serial patterns. *Psychology and Aging*, *12*, 634–656. https://doi.org/10.1037/0882-7974.12.4.634, PubMed: 9416632
Humphreys, G. F., Lambon Ralph, M. A., & Simons, J. S. (2021). A unifying account of angulargGyrus contributions to episodic and semantic cognition. *Trends in Neurosciences*, *44*, 452–463. https://doi.org/10.1016/j.tins.2021.01.006, PubMed: 33612312
Hung, Y. H., Frost, S. J., Molfese, P., Malins, J. G., Landi, N., Mencl, W. E., et al. (2019). Common neural basis of motor sequence learning and word recognition and its relation with individual differences in reading skill. *Scientific Studies of Reading*, *23*, 89–100. https://doi.org/10.1080/10888438.2018.1451533, PubMed: 31105422
Ito, M. (2008). Control of mental activities by internal models in the cerebellum. *Nature Reviews Neuroscience*, *9*, 304–313. https://doi.org/10.1038/nrn2332, PubMed: 18319727
Ivry, R. B., & Keele, S. W. (1989). Timing functions of the cerebellum. *Journal of Cognitive Neuroscience*, *1*, 136–152. https://doi.org/10.1162/jocn.1989.1.2.136, PubMed: 23968462
Janacsek, K., Ambrus, G. G., Paulus, W., Antal, A., & Nemeth, D. (2015). Right hemisphere advantage in statistical learning: Evidence from a probabilistic sequence learning task. *Brain Stimulation*, *8*, 277–282. https://doi.org/10.1016/j.brs.2014.11.008, PubMed: 25499036
Janacsek, K., Evans, T. M., Kiss, M., Shah, L., Blumenfeld, H., & Ullman, M. T. (2022). Subcortical cognition: The fruit below the rind. *Annual Review of Neuroscience*, *45*, 361–386. https://doi.org/10.1146/annurev-neuro-110920-013544, PubMed: 35385670
Janacsek, K., & Nemeth, D. (2012). Predicting the future: From implicit learning to consolidation. *International Journal of Psychophysiology*, *83*, 213–221. https://doi.org/10.1016/j.ijpsycho.2011.11.012, PubMed: 22154521
Janacsek, K., Shattuck, K. F., Tagarelli, K. M., Lum, J. A. G., Turkeltaub, P. E., & Ullman, M. T. (2020). Sequence learning in the human brain: A functional neuroanatomical meta-analysis of serial reaction time studies. *Neuroimage*, *207*, 116387. https://doi.org/10.1016/j.neuroimage.2019.116387, PubMed: 31765803
Karlaftis, V. M., Giorgio, J., Vértes, P. E., Wang, R., Shen, Y., Tino, P., et al. (2019). Multimodal imaging of brain connectivity reveals predictors of individual decision strategy in statistical learning. *Nature Human Behaviour*, *3*, 297–307. https://doi.org/10.1038/s41562-018-0503-4, PubMed: 30873437
Karuza, E. A., Li, P., Weiss, D. J., Bulgarelli, F., Zinszer, B. D., & Aslin, R. N. (2016). Sampling over nonuniform distributions: A neural efficiency account of the primacy effect in statistical learning. *Journal of Cognitive Neuroscience*, *28*, 1484–1500. https://doi.org/10.1162/jocn_a_00990, PubMed: 27315265
Keresztes, A., Ngo, C. T., Lindenberger, U., Werkle-Bergner, M., & Newcombe, N. S. (2018). Hippocampal maturation drives memory from generalization to specificity. *Trends in Cognitive Sciences*, *22*, 676–686. https://doi.org/10.1016/j.tics.2018.05.004, PubMed: 29934029
Kiss, M., Nemeth, D., & Janacsek, K. (2022). Do temporal factors affect whether our performance accurately reflects our underlying knowledge? The effects of stimulus presentation rates on the performance versus competence dissociation. *Cortex*, *157*, 65–80. https://doi.org/10.1016/j.cortex.2022.09.003, PubMed: 36274443
Kóbor, A., Horváth, K., Kardos, Z., Nemeth, D., & Janacsek, K. (2020). Perceiving structure in unstructured stimuli: Implicitly acquired prior knowledge impacts the processing of unpredictable transitional probabilities. *Cognition*, *205*, 104413. https://doi.org/10.1016/j.cognition.2020.104413, PubMed: 32747072
Kóbor, A., Horváth, K., Kardos, Z., Takács, Á., Janacsek, K., Csépe, V., et al. (2019). Tracking the implicit acquisition of nonadjacent transitional probabilities by ERPs. *Memory & Cognition*, *47*, 1546–1566. https://doi.org/10.3758/s13421-019-00949-x, PubMed: 31236822
Kóbor, A., Janacsek, K., Takács, Á., & Nemeth, D. (2017). Statistical learning leads to persistent memory: Evidence for one-year consolidation. *Scientific Reports*, *7*, 760. https://doi.org/10.1038/s41598-017-00807-3, PubMed: 28396586
Kóbor, A., Kardos, Z., Horváth, K., Janacsek, K., Takács, Á., Csépe, V., et al. (2021). Implicit anticipation of probabilistic regularities: Larger CNV emerges for unpredictable events. *Neuropsychologia*, *156*, 107826. https://doi.org/10.1016/j.neuropsychologia.2021.107826, PubMed: 33716039
Kóbor, A., Takács, Á., Kardos, Z., Janacsek, K., Horváth, K., Csépe, V., et al. (2018). ERPs differentiate the sensitivity to statistical probabilities and the learning of sequential structures during procedural learning. *Biological Psychology*, *135*, 180–193. https://doi.org/10.1016/j.biopsycho.2018.04.001, PubMed: 29634990
Krakauer, J. W., & Shadmehr, R. (2006). Consolidation of motor memory. *Trends in Neurosciences*, *29*, 58–64. https://doi.org/10.1016/j.tins.2005.10.003, PubMed: 16290273
Kurth, F., Zilles, K., Fox, P. T., Laird, A. R., & Eickhoff, S. B. (2010). A link between the systems: Functional differentiation and integration within the human insula revealed by meta-analysis. *Brain Structure & Function*, *214*, 519–534. https://doi.org/10.1007/s00429-010-0255-z, PubMed: 20512376
Landau, S. M., & D'Esposito, M. (2006). Sequence learning in pianists and nonpianists: An fMRI study of motor expertise. *Cognitive, Affective, & Behavioral Neuroscience*, *6*, 246–259. https://doi.org/10.3758/CABN.6.3.246, PubMed: 17243360
Leggio, M., & Molinari, M. (2015). Cerebellar sequencing: A trick for predicting the future. *Cerebellum*, *14*, 35–38. https://doi.org/10.1007/s12311-014-0616-x, PubMed: 25331541
Lewis, L. D., Setsompop, K., Rosen, B. R., & Polimeni, J. R. (2018). Stimulus-dependent hemodynamic response timing across the human subcortical-cortical visual pathway identified through high spatiotemporal resolution 7 T fMRI. *Neuroimage*, *181*, 279–291. https://doi.org/10.1016/j.neuroimage.2018.06.056, PubMed: 29935223
Ma, Q., Pu, M., Heleven, E., Haihambo, N. P., Baetens, K., Baeken, C., et al. (2021). The posterior cerebellum supports implicit learning of social belief sequences. *Cognitive, Affective, & Behavioral Neuroscience*, *21*, 970–992. https://doi.org/10.3758/s13415-021-00910-z, PubMed: 34100254
Magon, S., Pfister, A., Laura, G., Lüthi, M., Papadopoulou, A., Kappos, L., et al. (2020). Short timescale modulation of cortical and cerebellar activity in the early phase of motor sequence learning: An fMRI study. *Brain Imaging and Behavior*, *14*, 2159–2175. https://doi.org/10.1007/s11682-019-00167-8, PubMed: 31352651
Maheu, M., Meyniel, F., & Dehaene, S. (2022). Rational arbitration between statistics and rules in human sequence processing. *Nature Human Behaviour*, *6*, 1087–1103. https://doi.org/10.1038/s41562-021-01259-6, PubMed: 35501360
Margulies, D. S., Vincent, J. L., Kelly, C., Lohmann, G., Uddin, L. Q., Biswal, B. B., et al. (2009). Precuneus shares intrinsic functional architecture in humans and monkeys. *Proceedings of the National Academy of Sciences, U.S.A.*, *106*,

20069–20074. https://doi.org/10.1073/pnas.0905314106, PubMed: 19903877
Mugler, J. P., III., & Brookeman, J. R. (1990). Three-dimensional magnetization-prepared rapid gradient-echo imaging (3D MP RAGE). *Magnetic Resonance in Medicine*, *15*, 152–157. https://doi.org/10.1002/mrm.1910150117, PubMed: 2374495
Nemeth, D., & Janacsek, K. (2011). The dynamics of implicit skill consolidation in young and elderly adults. *Journals of Gerontology: Series B, Psychological Sciences and Social Sciences*, *66*, 15–22. https://doi.org/10.1093/geronb/gbq063, PubMed: 20929973
Nemeth, D., Janacsek, K., & Fiser, J. (2013). Age-dependent and coordinated shift in performance between implicit and explicit skill learning. *Frontiers in Computational Neuroscience*, *7*, 147. https://doi.org/10.3389/fncom.2013.00147, PubMed: 24155717
Nemeth, D., Janacsek, K., Londe, Z., Ullman, M. T., Howard, D. V., & Howard, J. H., Jr. (2010). Sleep has no critical role in implicit motor sequence learning in young and old adults. *Experimental Brain Research*, *201*, 351–358. https://doi.org/10.1007/s00221-009-2024-x, PubMed: 19795111
Nemeth, D., Janacsek, K., Polner, B., & Kovacs, Z. A. (2013). Boosting human learning by hypnosis. *Cerebral Cortex*, *23*, 801–805. https://doi.org/10.1093/cercor/bhs068, PubMed: 22459017
Oldfield, R. C. (1971). The assessment and analysis of handedness: The Edinburgh Inventory. *Neuropsychologia*, *9*, 97–113. https://doi.org/10.1016/0028-3932(71)90067-4, PubMed: 5146491
Ordin, M., Polyanskaya, L., & Soto, D. (2020). Neural bases of learning and recognition of statistical regularities. *Annals of the New York Academy of Sciences*, *1467*, 60–76. https://doi.org/10.1111/nyas.14299, PubMed: 31919870
Pan, S. C., & Rickard, T. C. (2015). Sleep and motor learning: Is there room for consolidation? *Psychological Bulletin*, *141*, 812–834. https://doi.org/10.1037/bul0000009, PubMed: 25822130
Park, J., Janacsek, K., Nemeth, D., & Jeon, H.-A. (2022). Reduced functional connectivity supports statistical learning of temporally distributed regularities. *Neuroimage*, *260*, 119459. https://doi.org/10.1016/j.neuroimage.2022.119459, PubMed: 35820582
Pelli, D. G. (1997). The VideoToolbox software for visual psychophysics: Transforming numbers into movies. *Spatial Vision*, *10*, 437–442. https://doi.org/10.1163/156856897X00366, PubMed: 9176953
Petro, L. S., & Muckli, L. (2016). The brain's predictive prowess revealed in primary visual cortex. *Proceedings of the National Academy of Sciences, U.S.A.*, *113*, 1124. https://doi.org/10.1073/pnas.1523834113, PubMed: 26772315
Poldrack, R. A., Sabb, F. W., Foerde, K., Tom, S. M., Asarnow, R. F., Bookheimer, S. Y., et al. (2005). The neural correlates of motor skill automaticity. *Journal of Neuroscience*, *25*, 5356–5364. https://doi.org/10.1523/JNEUROSCI.3880-04.2005, PubMed: 15930384
Power, J. D., Mitra, A., Laumann, T. O., Snyder, A. Z., Schlaggar, B. L., & Petersen, S. E. (2014). Methods to detect, characterize, and remove motion artifact in resting state fMRI. *Neuroimage*, *84*, 320–341. https://doi.org/10.1016/j.neuroimage.2013.08.048, PubMed: 23994314
Purdon, S. E., Waldie, B., Woodward, N. D., Wilman, A. H., & Tibbo, P. G. (2011). Procedural learning in first episode schizophrenia investigated with functional magnetic resonance imaging. *Neuropsychology*, *25*, 147–158. https://doi.org/10.1037/a0021222, PubMed: 21381822
Qian, T., Jaeger, T. F., & Aslin, R. (2012). Learning to represent a multi-context environment: More than detecting changes. *Frontiers in Psychology*, *3*, 228. https://doi.org/10.3389/fpsyg.2012.00228, PubMed: 22833727
Reber, P. J. (2013). The neural basis of implicit learning and memory: A review of neuropsychological and neuroimaging research. *Neuropsychologia*, *51*, 2026–2042. https://doi.org/10.1016/j.neuropsychologia.2013.06.019, PubMed: 23806840
Rey, A., Bogaerts, L., Tosatto, L., Bonafos, G., Franco, A., & Favre, B. (2020). Detection of regularities in a random environment. *Quarterly Journal of Experimental Psychology*, *73*, 2106–2118. https://doi.org/10.1177/1747021820941356, PubMed: 32640871
Rieckmann, A., Fischer, H., & Backman, L. (2010). Activation in striatum and medial temporal lobe during sequence learning in younger and older adults: Relations to performance. *Neuroimage*, *50*, 1303–1312. https://doi.org/10.1016/j.neuroimage.2010.01.015, PubMed: 20079855
Robertson, E. M., Pascual-Leone, A., & Miall, R. C. (2004). Current concepts in procedural consolidation. *Nature Reviews Neuroscience*, *5*, 576–582. https://doi.org/10.1038/nrn1426, PubMed: 15208699
Rolls, E. T., Huang, C.-C., Lin, C.-P., Feng, J., & Joliot, M. (2020). Automated anatomical labelling atlas 3. *Neuroimage*, *206*, 116189. https://doi.org/10.1016/j.neuroimage.2019.116189, PubMed: 31521825
Romano, J. C., Howard, J. H., Jr., & Howard, D. V. (2010). One-year retention of general and sequence-specific skills in a probabilistic, serial reaction time task. *Memory*, *18*, 427–441. https://doi.org/10.1080/09658211003742680, PubMed: 20408037
Rose, M., Haider, H., Salari, N., & Büchel, C. (2011). Functional dissociation of hippocampal mechanism during implicit learning based on the domain of associations. *Journal of Neuroscience*, *31*, 13739–13745. https://doi.org/10.1523/JNEUROSCI.3020-11.2011, PubMed: 21957237
Rosenthal, C. R., Andrews, S. K., Antoniades, C. A., Kennard, C., & Soto, D. (2016). Learning and recognition of a non-conscious sequence of events in human primary visual cortex. *Current Biology*, *26*, 834–841. https://doi.org/10.1016/j.cub.2016.01.040, PubMed: 26948883
Rosenthal, C. R., Mallik, I., Caballero-Gaudes, C., Sereno, M. I., & Soto, D. (2018). Learning of goal-relevant and -irrelevant complex visual sequences in human V1. *Neuroimage*, *179*, 215–224. https://doi.org/10.1016/j.neuroimage.2018.06.023, PubMed: 29906635
Roser, M. E., Fiser, J., Aslin, R. N., & Gazzaniga, M. S. (2011). Right hemisphere dominance in visual statistical learning. *Journal of Cognitive Neuroscience*, *23*, 1088–1099. https://doi.org/10.1162/jocn.2010.21508, PubMed: 20433243
Ross, R. S., Brown, T. I., & Stern, C. E. (2009). The retrieval of learned sequences engages the hippocampus: Evidence from fMRI. *Hippocampus*, *19*, 790–799. https://doi.org/10.1002/hipo.20558, PubMed: 19219919
Schapiro, A. C., Gregory, E., Landau, B., McCloskey, M., & Turk-Browne, N. B. (2014). The necessity of the medial temporal lobe for statistical learning. *Journal of Cognitive Neuroscience*, *26*, 1736–1747. https://doi.org/10.1162/jocn_a_00578, PubMed: 24456393
Schapiro, A. C., Kustner, L. V., & Turk-Browne, N. B. (2012). Shaping of object representations in the human medial temporal lobe based on temporal regularities. *Current Biology*, *22*, 1622–1627. https://doi.org/10.1016/j.cub.2012.06.056, PubMed: 22885059
Schapiro, A. C., Turk-Browne, N. B., Botvinick, M. M., & Norman, K. A. (2017). Complementary learning systems within the hippocampus: A neural network modelling approach to reconciling episodic memory with statistical learning. *Philosophical Transactions of the Royal Society of*

London, Series B: Biological Sciences, *372*, 20160049. https://doi.org/10.1098/rstb.2016.0049, PubMed: 27872368
Schendan, H. E., Searl, M. M., Melrose, R. J., & Stern, C. E. (2003). An fMRI study of the role of the medial temporal lobe in implicit and explicit sequence learning. *Neuron*, *37*, 1013–1025. https://doi.org/10.1016/S0896-6273(03)00123-5, PubMed: 12670429
Seghier, M. L. (2013). The angular gyrus: Multiple functions and multiple subdivisions. *Neuroscientist*, *19*, 43–61. https://doi.org/10.1177/1073858412440596, PubMed: 22547530
Sherman, B. E., & Turk-Browne, N. B. (2020). Statistical prediction of the future impairs episodic encoding of the present. *Proceedings of the National Academy of Sciences, U.S.A.*, *117*, 22760–22770. https://doi.org/10.1073/pnas.2013291117, PubMed: 32859755
Sherman, B. E., Turk-Browne, N. B., & Goldfarb, E. V. (2024). Multiple memory subsystems: Reconsidering memory in the mind and brain. *Perspectives on Psychological Science*, *19*, 103–125. https://doi.org/10.1177/17456916231179146, PubMed: 37390333
Shohamy, D., & Wagner, A. D. (2008). Integrating memories in the human brain: Hippocampal-midbrain encoding of overlapping events. *Neuron*, *60*, 378–389. https://doi.org/10.1016/j.neuron.2008.09.023, PubMed: 18957228
Smith, F. W., & Muckli, L. (2010). Nonstimulated early visual areas carry information about surrounding context. *Proceedings of the National Academy of Sciences, U.S.A.*, *107*, 20099–20103. https://doi.org/10.1073/pnas.1000233107, PubMed: 21041652
Song, S., Howard, J. H., Jr., & Howard, D. V. (2007). Sleep does not benefit probabilistic motor sequence learning. *Journal of Neuroscience*, *27*, 12475–12483. https://doi.org/10.1523/JNEUROSCI.2062-07.2007, PubMed: 18003825
Stark-Inbar, A., Raza, M., Taylor, J. A., & Ivry, R. B. (2017). Individual differences in implicit motor learning: Task specificity in sensorimotor adaptation and sequence learning. *Journal of Neurophysiology*, *117*, 412–428. https://doi.org/10.1152/jn.01141.2015, PubMed: 27832611
Stoodley, C. J., & Schmahmann, J. D. (2009). Functional topography in the human cerebellum: A meta-analysis of neuroimaging studies. *Neuroimage*, *44*, 489–501. https://doi.org/10.1016/j.neuroimage.2008.08.039, PubMed: 18835452
Stoodley, C. J., & Schmahmann, J. D. (2016). Functional topography of the human cerebellum. In D. L. Gruol, N. Koibuchi, M. Manto, M. Molinari, J. D. Schmahmann, & Y. She (Eds.), *Essentials of cerebellum and cerebellar disorders* (pp. 373–381). Springer. https://doi.org/10.1007/978-3-319-24551-5_51
Stoodley, C. J., & Schmahmann, J. D. (2018). Functional topography of the human cerebellum. In M. Manto & T. A. G. M. Huisman (Eds.), *Handbook of clinical neurology* (Vol. 154, pp. 59–70). Elsevier. https://doi.org/10.1016/B978-0-444-63956-1.00004-7, PubMed: 29903452
Szegedi-Hallgató, E., Janacsek, K., & Nemeth, D. (2019). Different levels of statistical learning—Hidden potentials of sequence learning tasks. *PLoS One*, *14*, e0221966. https://doi.org/10.1371/journal.pone.0221966, PubMed: 31536512
Szegedi-Hallgató, E., Janacsek, K., Vékony, T., Tasi, L. A., Kerepes, L., Hompoth, E. A., et al. (2017). Explicit instructions and consolidation promote rewiring of automatic behaviors in the human mind. *Scientific Reports*, *7*, 4365. https://doi.org/10.1038/s41598-017-04500-3, PubMed: 28663547
Szücs-Bencze, L., Fanuel, L., Szabó, N., Quentin, R., Nemeth, D., & Vékony, T. (2023). Manipulating the rapid consolidation periods in a learning task affects general skills more than statistical learning and changes the dynamics of learning. *eNeuro*, *10*. https://doi.org/10.1523/ENEURO.0228-22.2022, PubMed: 36792360
Takács, Á., Kóbor, A., Kardos, Z., Janacsek, K., Horváth, K., Beste, C., et al. (2021). Neurophysiological and functional neuroanatomical coding of statistical and deterministic rule information during sequence learning. *Human Brain Mapping*, *42*, 3182–3201. https://doi.org/10.1002/hbm.25427, PubMed: 33797825
Thomas, K. M., Hunt, R. H., Vizueta, N., Sommer, T., Durston, S., Yang, Y., et al. (2004). Evidence of developmental differences in implicit sequence learning: An fMRI study of children and adults. *Journal of Cognitive Neuroscience*, *16*, 1339–1351. https://doi.org/10.1162/0898929042304688, PubMed: 15509382
Török, B., Janacsek, K., Nagy, D. G., Orbán, G., & Nemeth, D. (2017). Measuring and filtering reactive inhibition is essential for assessing serial decision making and learning. *Journal of Experimental Psychology: General*, *146*, 529–542. https://doi.org/10.1037/xge0000288, PubMed: 28383991
Tóth, B., Janacsek, K., Takács, Á., Kóbor, A., Zavecz, Z., & Nemeth, D. (2017). Dynamics of EEG functional connectivity during statistical learning. *Neurobiology of Learning and Memory*, *144*, 216–229. https://doi.org/10.1016/j.nlm.2017.07.015, PubMed: 28803867
Tóth-Fáber, E., Nemeth, D., & Janacsek, K. (2023). Lifespan developmental invariance in memory consolidation: Evidence from procedural memory. *PNAS Nexus*, *2*, pgad037. https://doi.org/10.1093/pnasnexus/pgad037, PubMed: 36896125
Turk-Browne, N. B., Scholl, B. J., Chun, M. M., & Johnson, M. K. (2009). Neural evidence of statistical learning: Efficient detection of visual regularities without awareness. *Journal of Cognitive Neuroscience*, *21*, 1934–1945. https://doi.org/10.1162/jocn.2009.21131, PubMed: 18823241
Turk-Browne, N. B., Scholl, B. J., Johnson, M. K., & Chun, M. M. (2010). Implicit perceptual anticipation triggered by statistical learning. *Journal of Neuroscience*, *30*, 11177–11187. https://doi.org/10.1523/JNEUROSCI.0858-10.2010, PubMed: 20720125
Uddin, L. Q. (2015). Salience processing and insular cortical function and dysfunction. *Nature Reviews Neuroscience*, *16*, 55–61. https://doi.org/10.1038/nrn3857, PubMed: 25406711
Uddin, L. Q., Nomi, J. S., Hébert-Seropian, B., Ghaziri, J., & Boucher, O. (2017). Structure and function of the human insula. *Journal of Clinical Neurophysiology*, *34*, 300–306. https://doi.org/10.1097/WNP.0000000000000377, PubMed: 28644199
Vakil, E., Bloch, A., & Cohen, H. (2017). Anticipation measures of sequence learning: Manual versus oculomotor versions of the serial reaction time task. *Quarterly Journal of Experimental Psychology*, *70*, 579–589. https://doi.org/10.1080/17470218.2016.1172095, PubMed: 27042771
Vakil, E., Schwizer Ashkenazi, S., Nevet-Perez, M., & Hassin-Baer, S. (2021). Implicit sequence learning in individuals with Parkinson's disease: The added value of using an ocular version of the serial reaction time (O-SRT) task. *Brain and Cognition*, *147*, 105654. https://doi.org/10.1016/j.bandc.2020.105654, PubMed: 33246230
van den Heuvel, M. P., & Sporns, O. (2013). Network hubs in the human brain. *Trends in Cognitive Sciences*, *17*, 683–696. https://doi.org/10.1016/j.tics.2013.09.012, PubMed: 24231140
Van Overwalle, F., Manto, M., Cattaneo, Z., Clausi, S., Ferrari, C., Gabrieli, J. D. E., et al. (2020). Consensus paper: Cerebellum and social cognition. *Cerebellum*, *19*, 833–868. https://doi.org/10.1007/s12311-020-01155-1, PubMed: 32632709
Vetter, P., Bola, Ł., Reich, L., Bennett, M., Muckli, L., & Amedi, A. (2020). Decoding natural sounds in early "visual" cortex of

congenitally blind individuals. *Current Biology*, *30*, 3039–3044. https://doi.org/10.1016/j.cub.2020.05.071, PubMed: 32559449
Vetter, P., Smith, F. W., & Muckli, L. (2014). Decoding sound and imagery content in early visual cortex. *Current Biology*, *24*, 1256–1262. https://doi.org/10.1016/j.cub.2014.04.020, PubMed: 24856208
Vékony, T., Ambrus, G. G., Janacsek, K., & Nemeth, D. (2022). Cautious or causal? Key implicit sequence learning paradigms should not be overlooked when assessing the role of DLPFC (commentary on Prutean et al.). *Cortex*, *148*, 222–226. https://doi.org/10.1016/j.cortex.2021.10.001, PubMed: 34789384
Wagner, I. C., van Buuren, M., Kroes, M. C. W., Gutteling, T. P., van der Linden, M., Morris, R. G., et al. (2015). Schematic memory components converge within angular gyrus during retrieval. *eLife*, *4*, e09668. https://doi.org/10.7554/eLife.09668, PubMed: 26575291
Whitfield-Gabrieli, S., & Nieto-Castanon, A. (2012). Conn: A functional connectivity toolbox for correlated and anticorrelated brain networks. *Brain Connectivity*, *2*, 125–141. https://doi.org/10.1089/brain.2012.0073, PubMed: 22642651
Willingham, D. B., Salidis, J., & Gabrieli, J. D. (2002). Direct comparison of neural systems mediating conscious and unconscious skill learning. *Journal of Neurophysiology*, *88*, 1451–1460. https://doi.org/10.1152/jn.2002.88.3.1451, PubMed: 12205165
Wolford, G., Miller, M. B., & Gazzaniga, M. (2000). The left hemisphere's role in hypothesis formation. *Journal of Neuroscience*, *20*, RC64. https://doi.org/10.1523/JNEUROSCI.20-06-j0003.2000, PubMed: 10704518
Yang, J., & Li, P. (2012). Brain networks of explicit and implicit learning. *PLoS One*, *7*, e42993. https://doi.org/10.1371/journal.pone.0042993, PubMed: 22952624
Zeithamova, D., & Bowman, C. R. (2020). Generalization and the hippocampus: More than one story? *Neurobiology of Learning and Memory*, *175*, 107317. https://doi.org/10.1016/j.nlm.2020.107317, PubMed: 33007461
Zinszer, B., & Weiss, D. (2013). When to hold and when to fold: Detecting structural changes in statistical learning. *Proceedings of the Annual Meeting of the Cognitive Science Society*, *35*, 3858–3863.
Zolnai, T., Dávid, D. R., Pesthy, O., Nemeth, M., Kiss, M., Nagy, M., et al. (2022). Measuring statistical learning by eye-tracking. *Experimental Results*, *3*, e10. https://doi.org/10.1017/exp.2022.8